STRATIGRAPHY AND PALEODEPOSITIONAL INTERPRETATION OF THE LOWER NACATOCH FORMATION (MAASTRICHTIAN), ROBERTSON COUNTY, TEXAS

A Thesis

by

FRANK WAYNE SIMS III

Submitted to the Office of Graduate and Professional Studies of
Texas A&M University
in partial fulfillment of the requirements for the degree of

MASTER OF SCIENCE

Chair of Committee,	Thomas Olszewski
Committee Members,	Walter Ayers
	Michael Tice
Head of Department,	John Giardino

May 2014

Major Subject: Geology

ABSTRACT

The lower Nacatoch Formation of the Maastrichtian Navarro Group is considered to be a secondary target for energy companies exploring oil and gas reservoirs. Previous investigators of the northern and western sections of the Nacatoch Formation interpreted this unit to represent a variety of coastal depositional environments. However, investigations have been limited in the southern extent of the Nacatoch Formation, which has created a gap in the data. Well logs, drill cuttings, and core descriptions were gathered to create cross-sections and maps used to interpret geometries, sediment distribution, grain sizes, fauna, and internal stratigraphy of the lower Nacatoch. In the study area on the northwestern corner of Robertson County, Texas, the lower Nacatoch interval is composed of laminated sand and shale of variable thickness and has bar forms trending northwest to southeast. It is interpreted to represent a starved, shallow shelf storm-dominated transgressive ridge/bar deposit. Stratigraphic heterogeneity of the lower Nacatoch is significant because of the effects it has on the vertical and horizontal permeability, as well as, completion methods needed for optimal extraction.

DEDICATION

I would like to dedicate this thesis to all my parents, my wife, and my posterity. Without any of these, we cannot become what we are, be who we become, or preserve our life's works and memory.

ACKNOWLEDGEMENTS

I would like to thank my mother and step-father, Terri Mueller and William Mueller, for their unyielding dedication and support through my struggles in education and life during my childhood, and to my father and step-mother, Frank W. Sims Jr. and Wanda Sims for their support, which has guided me like a compass through my life. I would also like to thank my wife, Kimberli Jo Sims for her patience, love and understanding during this long journey and to my son, Shannon Sims along with my future posterity, for reminding me what this whole journey was about.

I would like to thank my committee chair, Dr. Thomas Olszewski, and my committee members, Dr. Ayers, and Dr. Tice, for their guidance and support throughout the course of this research. Their counsel has been invaluable in this endeavor and I am grateful for their support to obtain a life's long dream.

I would like to thank Tammy Hinojos, Melanie Guthrie, Debra Boettger and the management team at NeuraLog Inc. for their support by use of their software suite during my research. Without the equipment and software this task would have been more difficult at best.

Finally, I would like to thank my friends and colleagues and the department faculty and staff for making my time at Texas A&M University a great experience. I also want to extend my gratitude to the Kelly Fellowship through the Berg-Hughes Foundation, and to Dr. Michael Pope, Dr. Zoya Heidari, and Dr. Thomas Yancey for all of the time spent assisting and working with me for higher understanding of my studies.

NOMENCLATURE

BEG	Bureau of Economic Geology
DP	Density Porosity
(ft)	Feet
GR	Gamma Ray
(km)	Kilometers
LLC	Limited Liability Company
LST	Low Stand Systems Tract
(m)	Meters
NP	Neutron Porosity
PEF	Photoelectric Factor
RS	Resistivity
RohB	Bulk Density
SP	Spontaneous Potential
TST	Transgressive System Tract

TABLE OF CONTENTS

LIST OF FIGURES

I. INTRODUCTION

The Maastrichtian age Navarro Group is a valuable hydrocarbon-producing interval in central Texas. Production is primarily from sandstones that were deposited in nearshore and shallow marine environments that have been interpreted to represent tidal flats, deltas, barrier islands, and shelf sand plumes (McGowen and Lopez, 1983; Condon and Dyman, 2006; Patterson and Scott, 1984; Bain, 2004). However, the depositional environment and stratigraphic architecture of the lower Nacatoch Formation has not been studied previously in the subsurface near its southern perimeter where it pinches out. Understanding the reservoir-scale geology of this unit is necessary to optimize hydrocarbon development in this area.

Calvert field in Robertson County, Texas (Figures 1 and 2) was discovered in 1944 by Hammond Oil Company. The area was first explored for oil and gas prospects in the Edwards Limestone but proved fruitless after five wells were drilled with no oil or gas shows. The lower Nacatoch Formation's productivity in the area was discovered during the drilling to the Edwards Limestone, but it was considered a secondary target. After wells were drilled to the Edwards Limestone in Calvert field, they were plugged back and completed in the Nacatoch. The Nacatoch Formation is responsible for approximately 1.2 MMbbl. of oil production from 1944 to 2007 (Texas State Railroad Commission, 2006).

The main goals of this study were to define depositional geometries, stratigraphic architecture, and paleodepositional environments of the lower Nacatoch interval in the Navarro Group in the Calvert field area. The regional study area includes Bell, Falls,

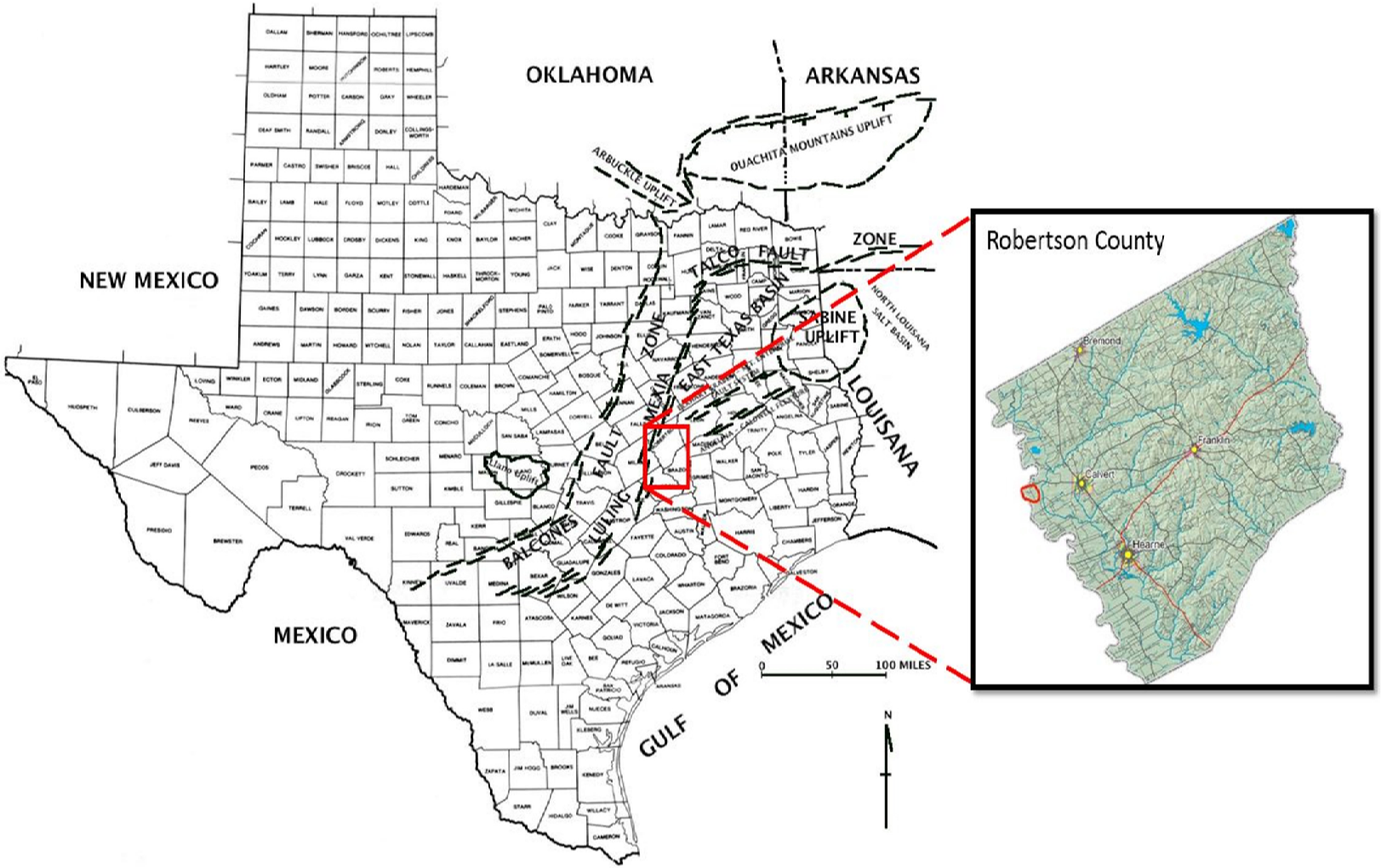

Figure 1. Geographical location of regional study area (outlined in red square). Texas counties picture modified from Texas Tech University (2012); structural features modified from McGowen and Lopez (1983).

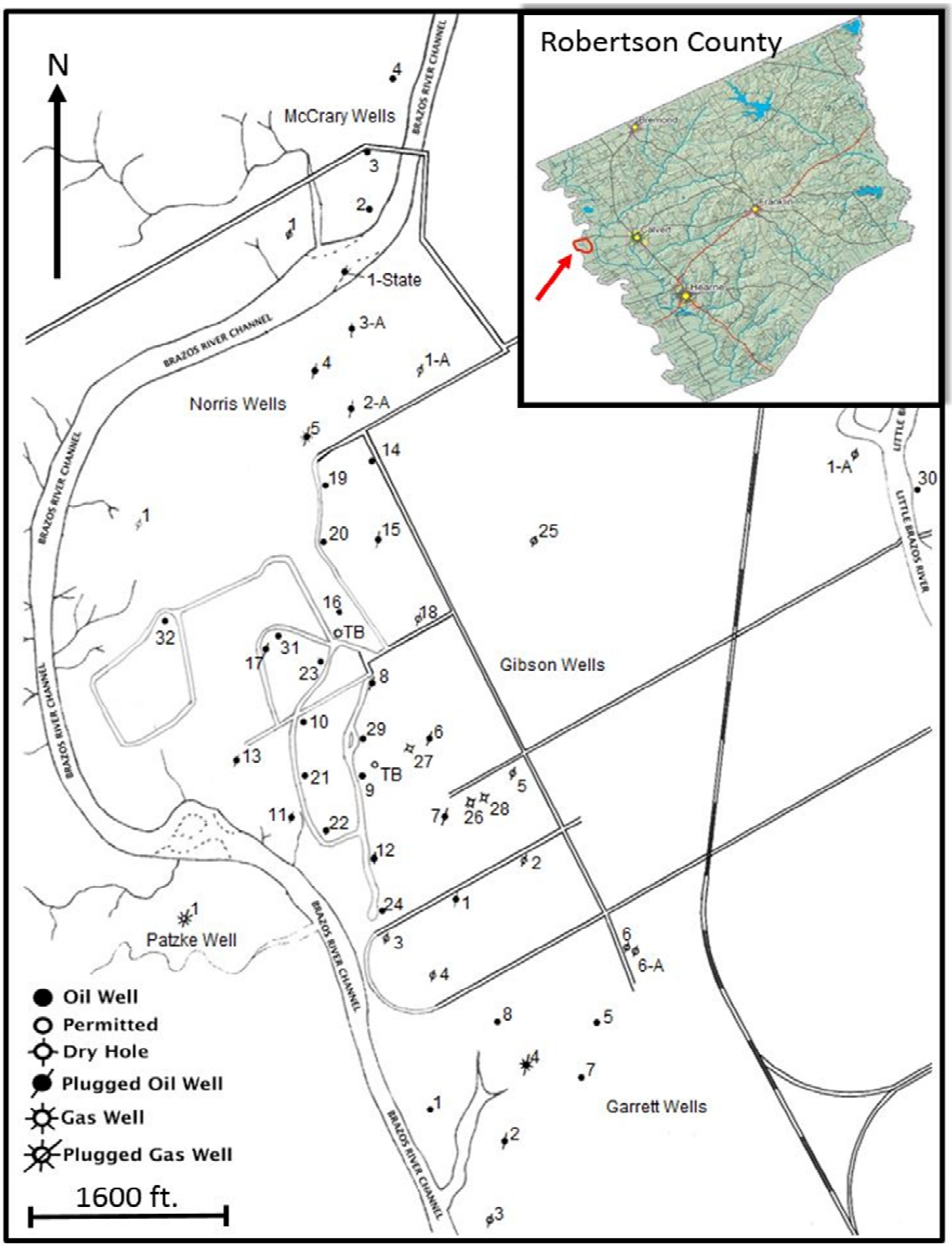

Figure 2. Specific study area in Robertson County, Texas. Calvert field (outlined in red in top right) is the conglomeration of McCrary, Norris, Gibson, Garrett and Patzke wells. Modified from Texas Tech University (2012).

Lee, Milam, and Robertson counties in Texas and covers 1,024 square miles (Figure 1). The detailed study area (Figure 2) encompasses a total of 5 square miles, which includes the productive Nacatoch Sandstone (Figure 3).

The working hypothesis, based on previous work, is that the lower interval of the Nacatoch Formation was deposited as a set of middle to outer shelf bars with a northeast to southwest strike orientation (McGowen and Lopez, 1983; Condon and Dyman, 2006; Patterson and Scott, 1984; Bain, 2004). In Calvert field, the lower Nacatoch interval is less than 20 feet thick and is interbedded sand and shale with offshore faunal assemblages, broken shell fragments, pyrite, glauconite and sand beds that do not exceed more than 3 ft. in thickness. However, stratigraphic geometries and internal structure of the lower Nacatoch interval in the study area do not match some of the previous descriptions reported from outcrops to the north and west and need further study.

Access to previously unavailable wireline logs, recent drill cuttings, and archived core descriptions provide an opportunity for a new and more complete understanding of the Navarro Group in the study area, resulting in a refined reconstruction of the paleodepositional environment of the Nacatoch Formation.

II. BACKGROUND AND PREVIOUS STUDIES

II.1 LITHOSTRATIGRAPHIC NOMENCLATURE AND DESCRIPTION

The Navarro Group is composed of interbedded sandstone and shale that tends to coarsen upwards within packages, although the overall grain size decreases stratigraphically upwards, indicating long term transgression (Bain, 2004; Knight et.al., 1984; Condon and Dyman, 2006). The Navarro Group is divided into the Lower Navarro Formation (Neylandville Marl), Nacatoch Sandstone (Nacatoch Formation), Upper Navarro Marl (Corsicana Marl), and the Upper Navarro Clay (Kemp Clay). The base of the Neylandville Marl (bottom of the Navarro Group) is an inferred unconformity defined by a phosphatic, glauconitic band and sandy marl (McGowen and Lopez, 1983). The Nacatoch Formation within the Navarro Group is composed of well-sorted, fine-to medium-grained, calcitic and glauconitic sandstones. Located between the Nacatoch Sand and the Corsicana Marl is a phosphatic band. The interface between the Corsicana Marl and Kemp Clay in the north is recorded as a minor erosional break (Stephenson, 1941). The interface between the Navarro Group and the overlying Midway Group marks the Cretaceous-Tertiary boundary and was recorded as an unconformity (Stephenson, 1941) (Figure 3).

II.2 NAVARRO GROUP FAUNAL ASSOCIATIONS

Fauna in the Navarro Group includes 411 species, over half of which (245 species) were found in the Nacatoch Formation (Stephenson, 1941). Where fossils are observed, the preservation was noted to be extremely good. The well-preserved fossils are found in concretions; other locations, however, are completely devoid of fossils,

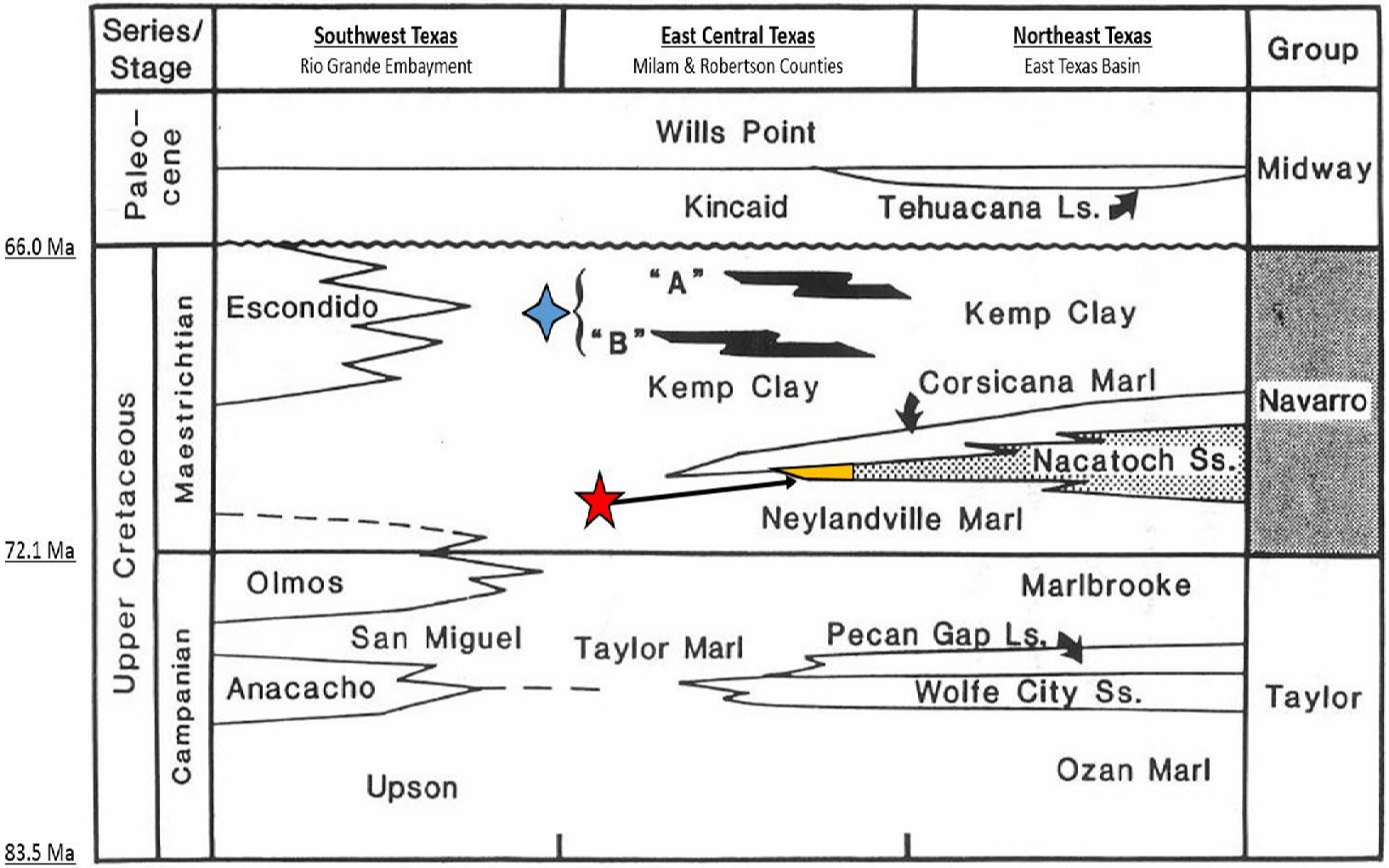

Figure 3. Lithostratigraphic nomenclature across Texas including study area. Nacatoch Formation (Nacatoch Sandstone) extent (5 pointed Red Star) across Texas and in relation to Patterson's work on the Navarro Sands A and B (4 pointed Blue Star) Modified from Patterson (1983).

which could suggest unfavorable conditions for organisms or lack of preservation. Stephenson (1941) suggests that marine fossils of the Nacatoch could represent transported allochthonous associations.

II.3 REGIONAL STRUCTURAL FRAMEWORK

Supercontinental breakup in the Proterozoic resulted in the formation of three failed continental rift junctions in the location of the present Gulf of Mexico. These are known today as the Delaware rift (Texas lineament) along the Rio Grande River, Reelfoot rift (Mississippi lineament) along the Mississippi River, and Southern Oklahoma aulacogen (Wichita lineament) along the Red River. Beginning in the Pennsylvanian, continental coalescence formed the supercontinent Pangea, resulting in the Ouachita and Marathon uplifts. Between these two uplifted sections is the Llano Uplift and its subsurface extension, the San Marcos Arch. At the end of the Triassic, Pangea began to break up and rift basins opened, resulting in the formation of the Gulf of Mexico. In the Middle Jurassic, the Louann Salt was deposited in the rift valleys. Finally, in the Late Cretaceous sea level rose to form the Western Interior Seaway.

The study area is in the East Texas Basin, bounded by the Llano Uplift and San Marcos Arch to the south and west and by the Sabine Uplift to the north and east (Condon and Dyman, 2006). The structural architecture of both the East Texas Basin and the research area has been influenced by the Luling-Mexia-Talco Fault Zone (Figure 1), which formed as the result of downdip migration of the Middle Jurassic Louann Salt into the Gulf of Mexico. The Luling-Mexia-Talco Fault Zone is a series of en echelon normal faults and grabens that displace Mesozoic to Eocene strata, including the Navarro Group.

Salt features were identified impacting the overlying structure of the Navarro Group where the Nacatoch appears to be thicker (McGowen and Lopez, 1983). This suggests co-eval faulting with the salt features during deposition of the Navarro Group.

II.4 REGIONAL DEPOSITIONAL FRAMEWORK

During the Maastrichtian the East Texas Basin was a complex coastal zone (Figure 4) with a paleo-shoreline trajectory trending northeast to southwest (Rainwater, 1960; McGowen and Lopez, 1983; Goldhammer and Johnson, 2001; Galloway, 2008).

Sea-level curves (Haq et. al., 1988; Miller et. al., 2005; Snedden, 2010) characterize the Maastrichtian as a time of eustatic sea level rise (Figure 5). It is hypothesized that the depositional environment to the west of the research area was deltaic, deriving its sediment from the north and west (McGowen and Lopez 1983). Also, the absence of Florida to the east allowed waves and current circulation from the Atlantic Ocean to have a much greater influence on the Gulf Coast than observed today. Consequently, the effect of longshore currents was greater on sediment deposition compared to the present-day Texas coast. The longshore currents are hypothesized to travel in the southwest direction along the coast similar to the present day trend (McGowen and Lopez 1983).

II.5 PREVIOUSLY INTERPRETED DEPOSITIONAL SETTING

In the northern East Texas Basin, the Nacatoch Formation has been interpreted as tidal flats and barrier island complexes based on the presence of bi-directional crossbeds and alternating lenticular and wavy bed sets (McGowen and Lopez 1983). Outcrop sections show fine to medium-grained, cross-bedded sand with individual foresets

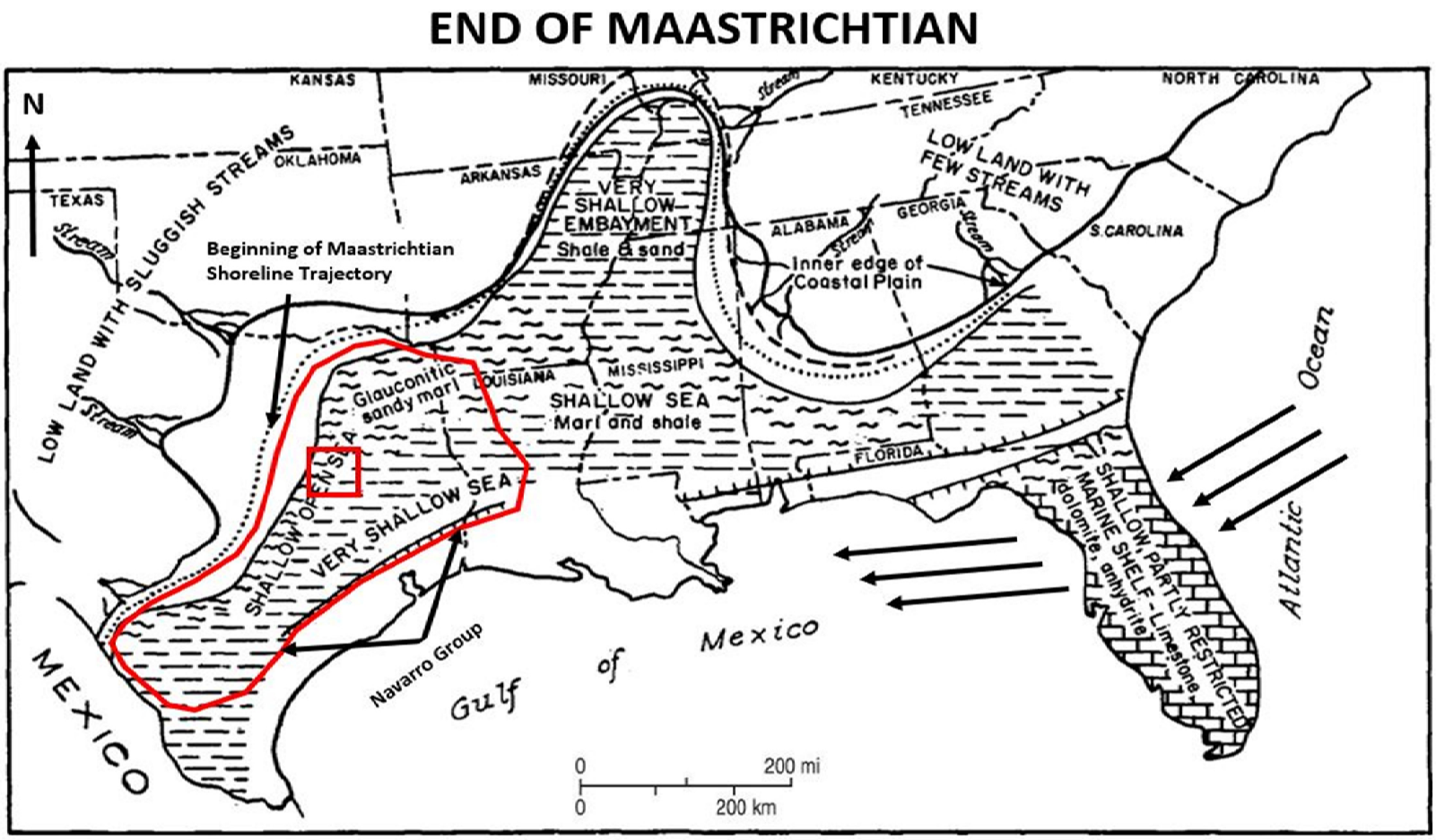

Figure 4. End of Maastrichtian paleogeography. Texas, Mexico and Gulf Coast paleogeography, depositional environments, and paleo-shoreline trajectory during the Maastrichtian in relationship to study area (red square). Area highlighted by irregular red outline indicates approximate Navarro Group extent. Three arrows indicate waves and current circulation across Florida due to absence of land mass above water. Modified from Rainwater (1960).

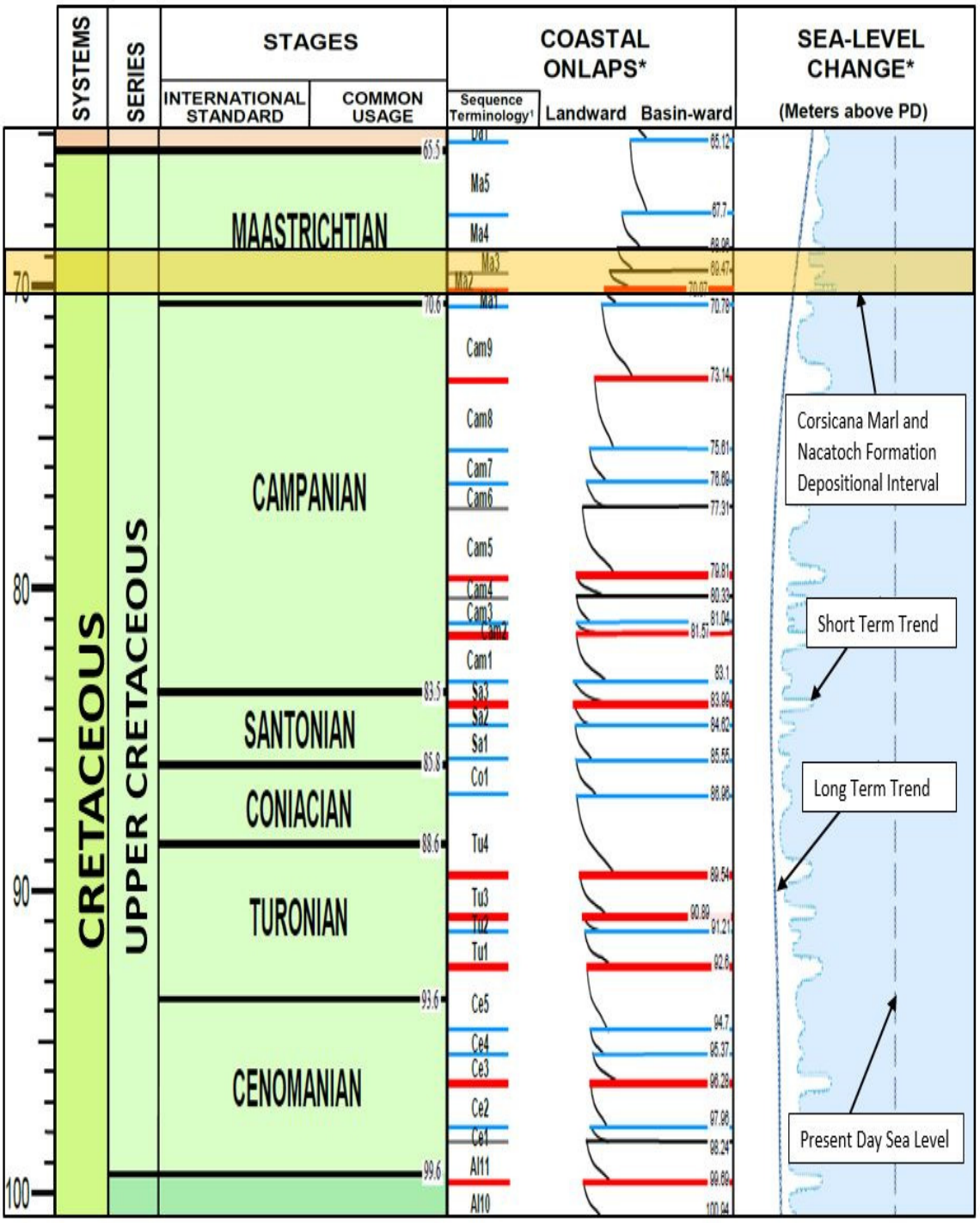

Figure 5. Sea level and onlap curves for the Upper Cretaceous. Red lines indicate sea-level change > 75 m, Black lines indicate sea-level change 25-75 m, Blue lines indicate sea-level change < 25 m. Modified from Snedden (2010).

ranging from 3 to 12 inches with mud clasts and pellets on the foresets. Current-rippled sand bodies have clay drapes, which also may indicate tidal influence. These clay drapes were interpreted to represent deposition between the ebb and flood of a tidal cycle, which suggested this was a tidal flat environment. In this outcrop area, lower shoreface deposits to the east of the tidal flats are cut by a channel fill, which could indicate migration of a barrier island (McGowen and Lopez 1983).

In the western part of the East Texas Basin, the Nacatoch Formation was interpreted as a deltaic complex based on inferred crevasse-splay deposits at the outcrop. The base of the succession has well-developed trough cross-bedding that indicates unidirectional flow and could be a small distributary. It is overlain by very fine-grained sandstones with heavy burrowing. The upper part is described as bioturbated, muddy, fine-grained sand with plant fragments up to 6mm in length (McGowen and Lopez 1983).

In the central East Texas Basin, the Nacatoch Formation was interpreted as a shelf sand plume complex formed by longshore currents that carried sand from the deltas out to sea (Patterson, 1983). Deposition of the sand was located approximately 21 to 40 miles from the shoreline and had approximate thicknesses of 3-20 feet. The shelf sand plume interpretation is based on inferred down-current, stratigraphic climbing shelf sand bar complexes. Shelf sand plume deposits of the Nacatoch Formation were interpreted to reflect rapid deposition (immature plume), abandonment (current reworked plume) and storm-modification (onshore reworked plume) (Patterson, 1983).

Finally, in the far southwest on the United States-Mexico border in Webb and Zapata Counties, Texas, the basal Navarro Group sands are approximately 15ft to 20ft thick. These sands, located throughout the Navarro Group and including the Nacatoch Formation, were described as deep water turbidities that represent a basin floor sand derived from the Olmos Delta Complex (Bain, 2004).

III. METHODS AND RESULTS

III.1 FORMATION IDENTIFICATION AND EVALUATION

Well logs, drill cuttings, and old core descriptions were utilized to develop a paleodepositional model and to understand the stratigraphic context of the lower Nacatoch interval in the study area.

III.1.1 Well Logs

Well logs in this study were used to identify, correlate and spatially constrain the units of the Navarro Group in the subsurface.

III.1.1.a Well Log Data Set

The lower Nacatoch interval in the study area was described based on 49 wells logs from the Calvert field (Figure 6 and 7) and an additional 23 well logs from the surrounding area acquired from the Bureau of Economic Geology (BEG). Old well log data (1940 – 1980) accounted for 52 wells, of which 49 were situated in the Calvert field study area. Two new wells were drilled in 2011 and 2013 by Talus Resources LLC. Twenty-three wells obtained from the BEG were used to expand cross-sections across the region. Old well log data consisted of resistivity and spontaneous potential measurements. Well logs obtained from the BEG consisted of gamma ray, spontaneous potential, resistivity, and neutron porosity. Well logs donated by Talus Resources LLC consisted of spontaneous potential, resistivity, gamma, neutron porosity, density porosity and photoelectric factor (PEF).Well logs were all converted to a 2” = 100’ scale.

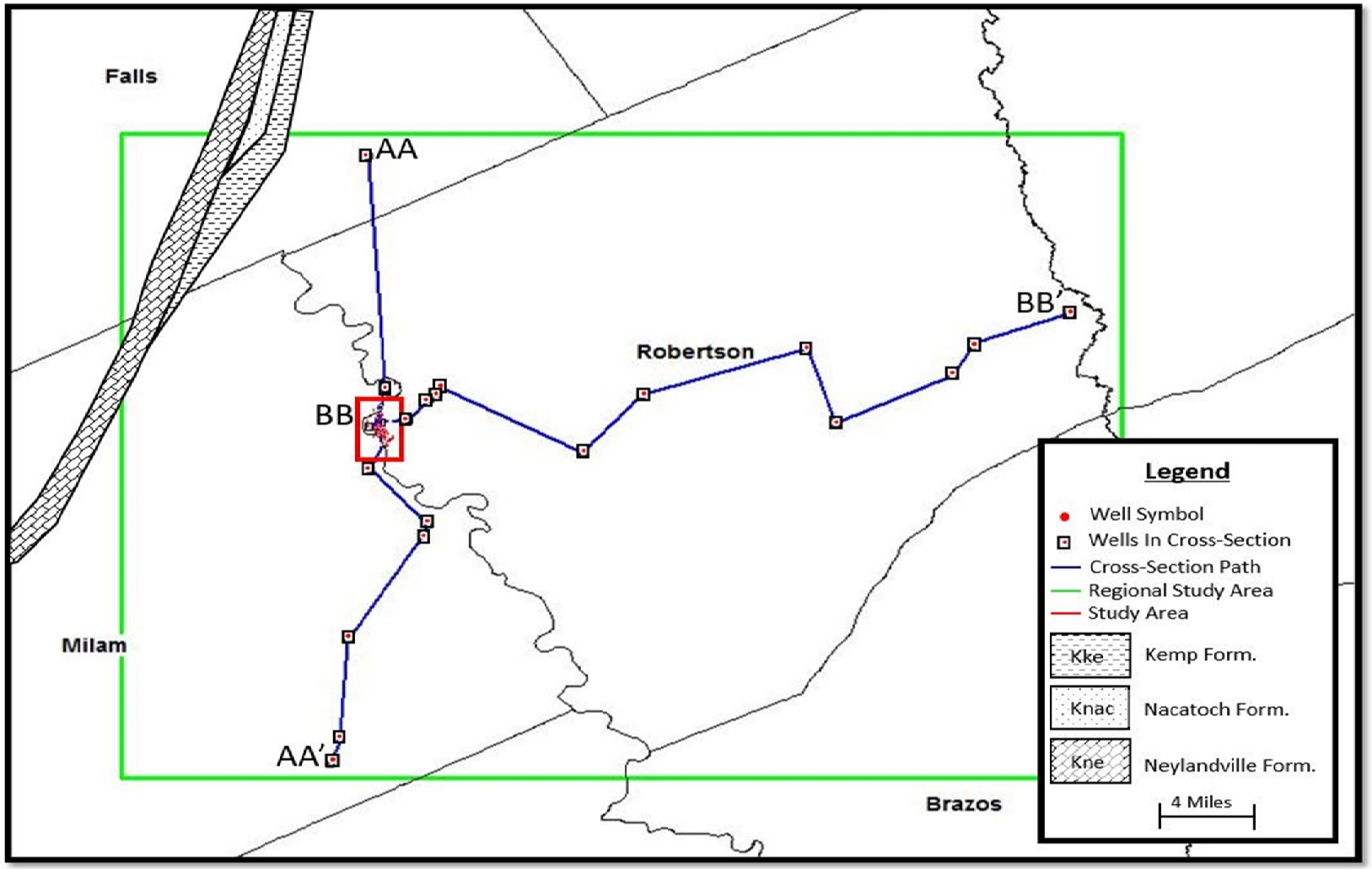

Figure 6. Regional cross-sections and approximate outcrop belt. Wells used in study are red, wells used in regional cross-sections are red with a black square.

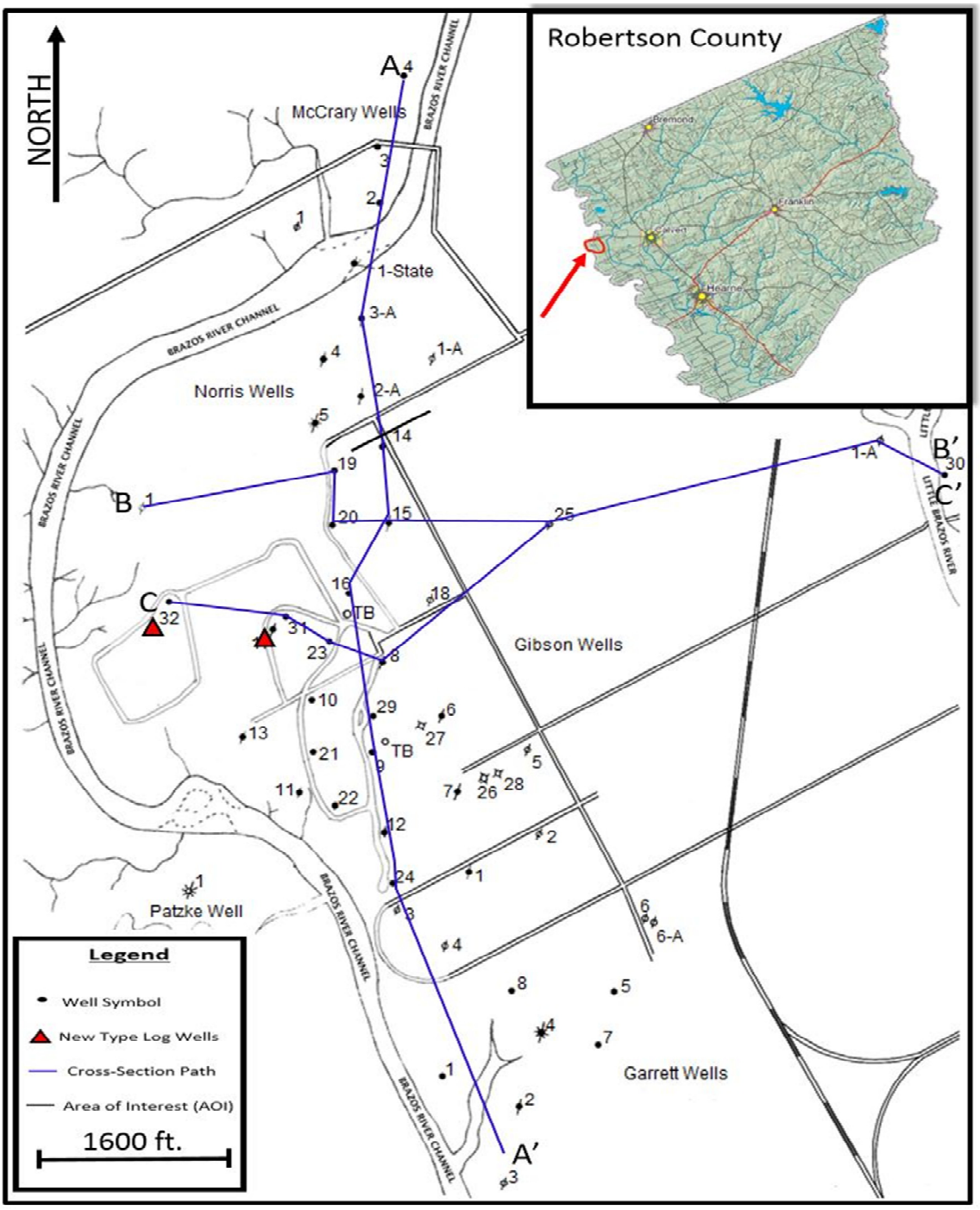

Figure 7. Cross-sections through study area. Wells used in study area in black. Wells with triangle shapes are Well Logs obtained in 2010 and 2012 for type logs. A to A' is a strike oriented cross-section (Fig.12) and B to B' is a dip oriented cross-section (Fig13). C to C' is the dip oriented structural cross-section. Calvert field and well locations outlined in red (Top Right). Modified from Texas Tech University (2012).

III.1.1.b Well Log Quality Control

Forty-nine well logs (old well logs) in the original data set were digitized at 400 DPI in black and white. All the well logs were scanned into the NeuraLog software package, where they were calibrated and manually manipulated to ensure proper transfer of information from physical logs to digital LAS files. The digitized logs were imported into the program and set on a virtual light table where a depth grid was generated. The depth grid was transposed on top of the corresponding depth markers in the imported image. The log curves in each track were individually traced from the digitized physical log. After the process was finished, the logs were converted to LAS files. The quality control of each log represents a value of consistency between the overlain digital lines on the light table compared to the lines on the imported log image for each track before conversion to an LAS file. Quality control reports were generated for each well log and ranged between 100% overlay to 67% overlay with a 97% average. This ensures there was minimal distortion from the physical paper logs to their digital representation.

III.1.1.c New Well Log Data

New well logs were obtained during the drilling operations of the Gibson #32 well in 2011 and the Gibson #31 well in 2013. Facies descriptions from well cuttings were matched to the new log from the Gibson #31 well, which was correlated to the Gibson #32 well 1,600 feet to the east (Figure 8). Once the stratigraphic correlation was established between the two new logs, they were used as type logs (Figures 7 and 8) to interpret the rest of the old well logs in the study area. The modern well logs (with modern tools in addition to SP and RS) were used to pick the stratigraphic surfaces on

older logs with more confidence.

III.1.1.d Well Log Interpretation Background

Logging tools have a radial depth of investigation, which represents the limited distance into the formation a logging tool can record data. The ability to resolve data properly with a logging tool is finite and can be compromised by many factors down hole, which makes it essential to use multiple logs to get the highest accuracy for each interval of interest.

Resistivity logs record the ability of fluids to conduct electricity. Noticeable change could represent mud-invaded zones, hydrocarbon presence, porosity and/or permeability changes. Mud properties and resistivity can change from well to well (McCubbin, 1981).

Spontaneous potential (SP) shows a positive or negative deflection when responding to changes in connate water and drilling mud. SP log negative deflection suggests that connate water resistivity is less than the mud filtrate resistivity ($R_w < R_{mf}$) and a positive deflection indicates the opposite. Deflection can be attributed to hydrocarbon presence, mud filtrate invasion, change in connate water properties, or permeability and porosity changes (McCubbin, 1981).

Gamma-ray (GR) logs are passive tools that record the intensity of natural radiation that is emitted by sediments. Most clays and shales have elements like potassium that emit low amounts of radiation that are typically absent in quartz sandstones and carbonates (Bassiouni, 1994).

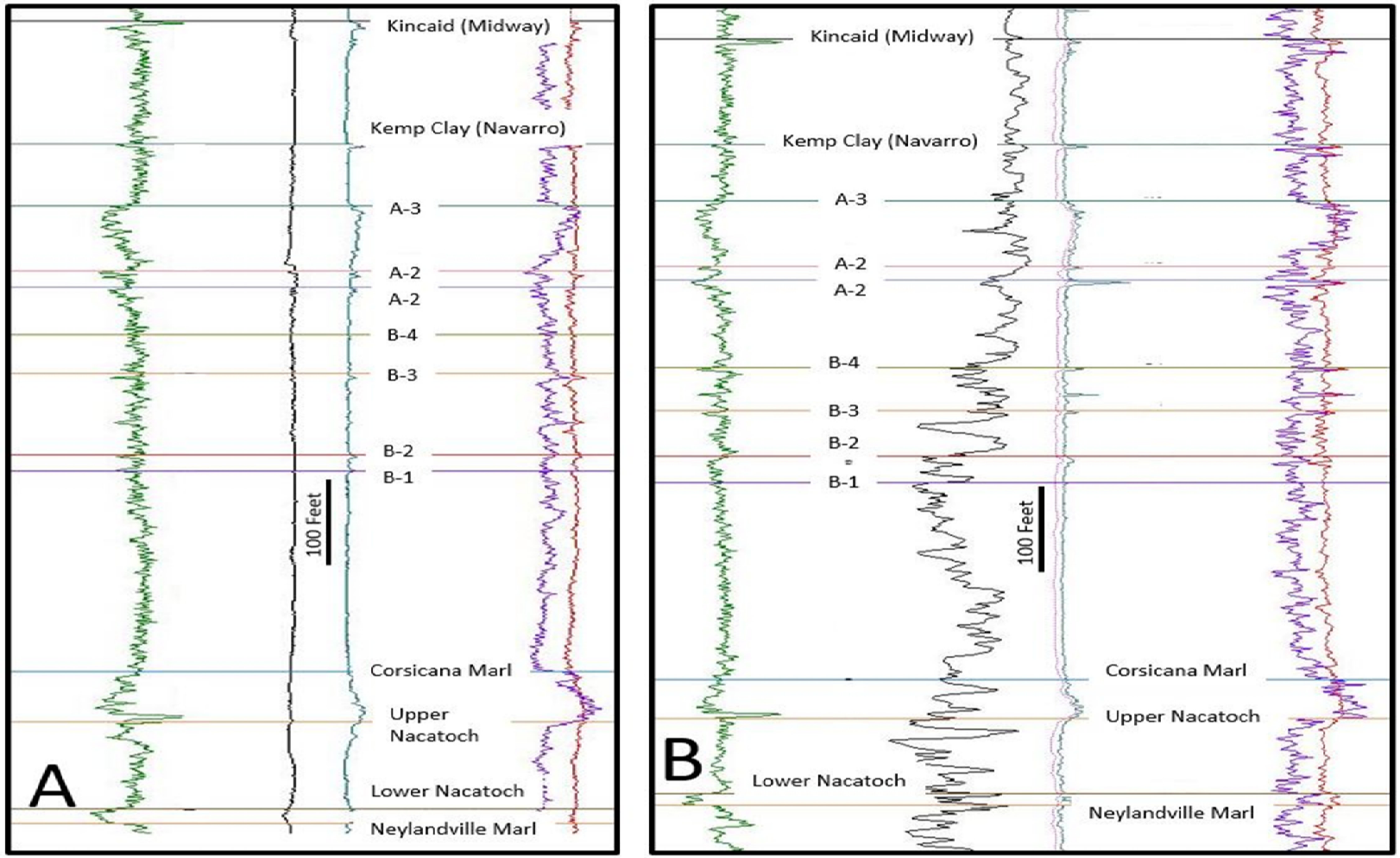

Figure 8. Log curves used to identify stratigraphy in study area. **(A)** Gibson #31 type log curves dark green (GR), black (SP), light green (Resistivity), pink (PEF), red (RhoB). **(B)** Gibson #32 type Log with surfaces corrected from Gibson #31 type log.

Photoelectric Effect (PEF) is an active tool that emits gamma radiation and excites atoms in the sediment. When energy emitted exceeds an electron's binding energy, it releases a photon that gives a specific signature for different types of minerals (Bassiouni, 1994).

III.1.1.e Well Log Results

Figure 9 compares well logs used in different studies of the Navarro interval. The datum used for correlation in this study was the upper surface of the Corsicana Marl, a lime rich mud that overlies the Nacatoch Formation. The Corsicana Marl was identified on logs by low GR response, no deflection on SP logs, relatively high RS, a bulk density of 2.7 to 2.75 (g/cm^3) and a PEF value > 4.0 (b/e) (Figure 8). This datum is well defined and extremely consistent throughout the study area. The upper Nacatoch interval was identified on logs by high GR response, negative to no deflection on SP logs, a bulk density of 2.1 to 2.4 (g/cm^3), and relatively low RS. The lower Nacatoch interval was identified on logs by low GR response, negative deflection on SP logs, a bulk density of 2.4 to 2.65 (g/cm^3), and a PEF value between 1.8 and 2.0 (b/e).

III.1.1.f Well Log Interpretation

Log curve shapes can be a diagnostic tool to indicate changes in depositional conditions (Pirson, 1981 and Rider, 1996) and are used to diagnose depositional environments, position on the shelf, and the sea-level events by comparing log shape geometries (Figure 10A and 10B). In open marine depositional environments, fining-upwards sedimentary successions are generally interpreted to represent transgression,

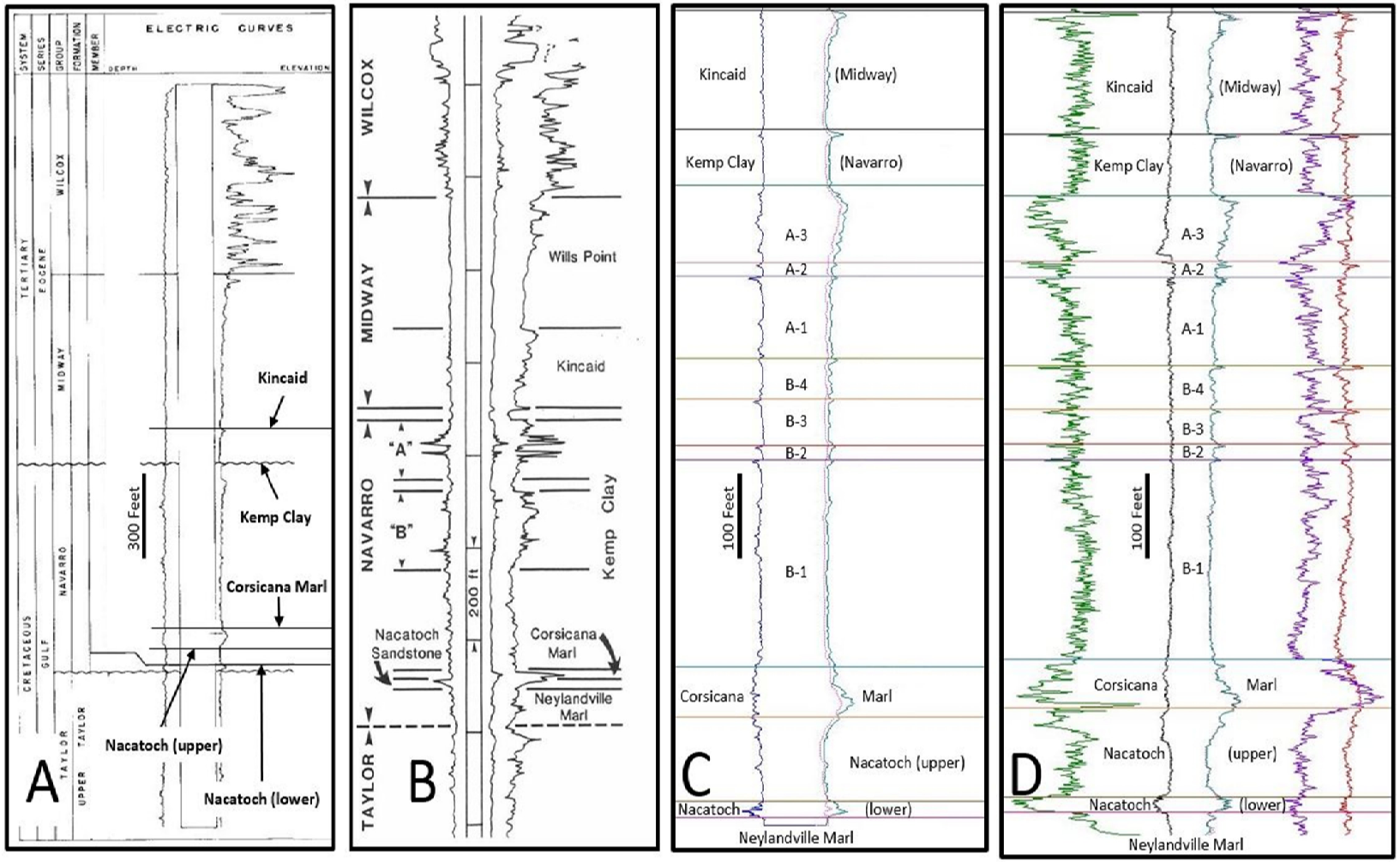

Figure 9. Type logs used for correlation in study area. **(A)** Type log used by Hammond Oil Co. in 1940s using SP and Resistivity (formation tops indicated by arrows). **(B)** Type log used by Patterson (1983) using SP and Resistivity. **(C)** Type log used in this study based on Gibson #21. **(D)** New Log of Gibson #31 drilled in 2013.

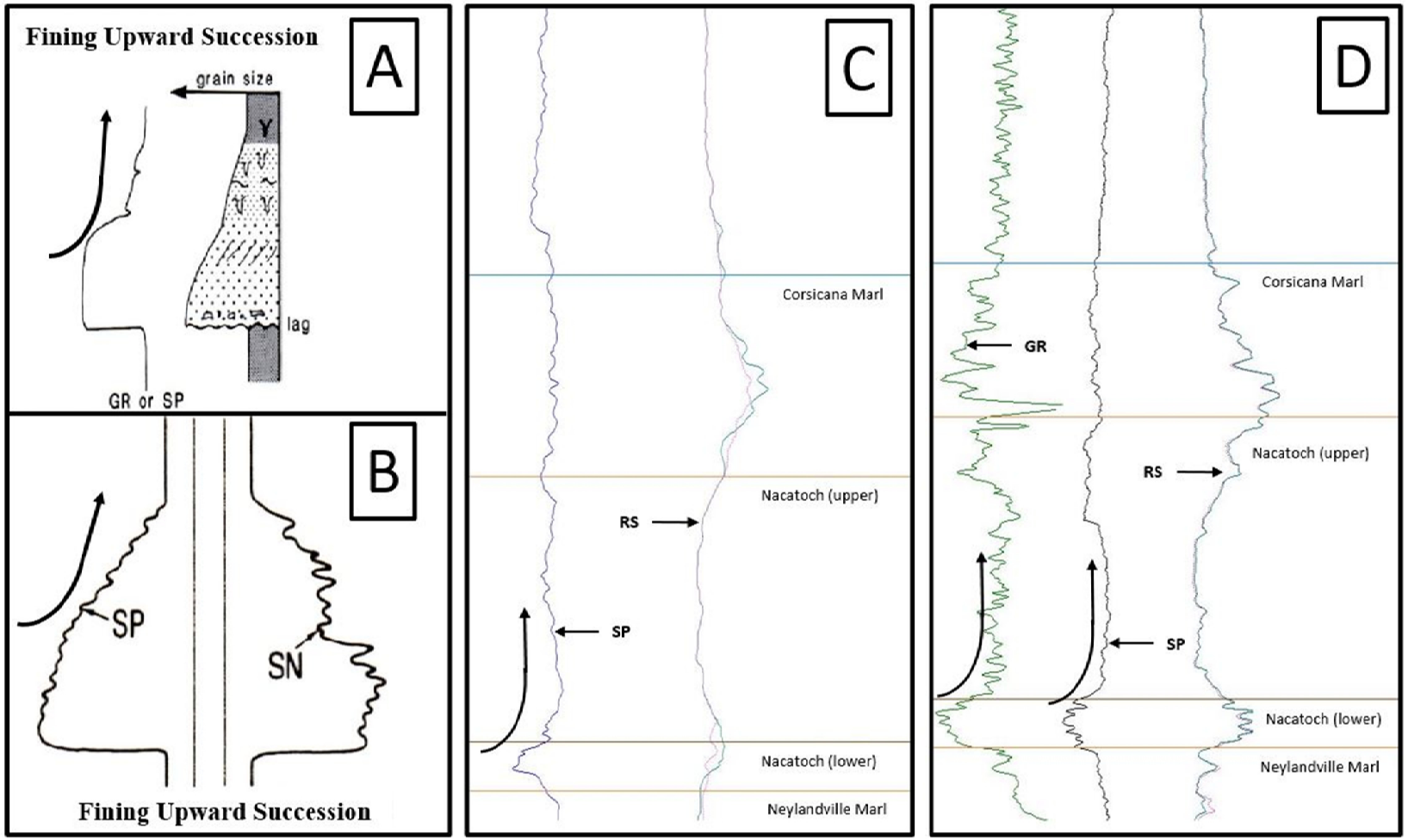

Figure 10. Well logs compared to interpretation schemes for transgressive sediments. Study area logs indicate a transgressive event. **(A)** Log geometries interpreted for marine transgressive sediment (Rider, 1996) (Modified). **(B)** Log geometries interpreted for transgressive sediment. (Modified from Pirson, 1981). **(C)** Gibson #27 blue (SP), teal (Shallow RS), pink (Deep RS). **(D)** Gibson #31 Type log curves green (GR), and black (SP).

whereas coarsening upwards represents regression.

Well logs from the base of the lower Nacatoch to the upper surface of the Corsicana Marl are interpreted as a fining upward succession (Figure 10C and 10D), suggesting an increase in water depth in the study area. Furthermore, well log evaluation, based on log geometries, can help constrain where sediments were deposited on a shelf (Pirson, 1981 and Rider, 1996). These sands are interpreted to represent sediment of a middle to outer shelf paleodepositional environment.

III.1.2 Cross-Sections

Cross-sections in this study were created to understand the vertical and lateral variation of stratigraphic thickness in the Nacatoch Formation. Cross-sections also indicate the lateral continuity of the Nacatoch Formation in the study area.

III.1.2.a Cross-Section Generation

Nine regional cross-sections were created but the focus was directed on the study area cross-sections due to poor quality of some logs for the region. Thirty four cross-sections of the study area were constructed: 12 strike-oriented and 13 dip-oriented. The cross-sections (Figures 11 A&B and 12 A&B) are set at geo-proportional spacing and the datum used was the top of the Neylandville Marl.

III.1.2.b Cross-Section Results

The Corsicana Marl interval maintains a thickness of 40-60 ft (12-18 m) in the study area with most of the thickening to the east. The upper Nacatoch interval ranges from 108 ft (33 m) in the north to 70 ft (21 m) in the south. The upper Nacatoch thins in

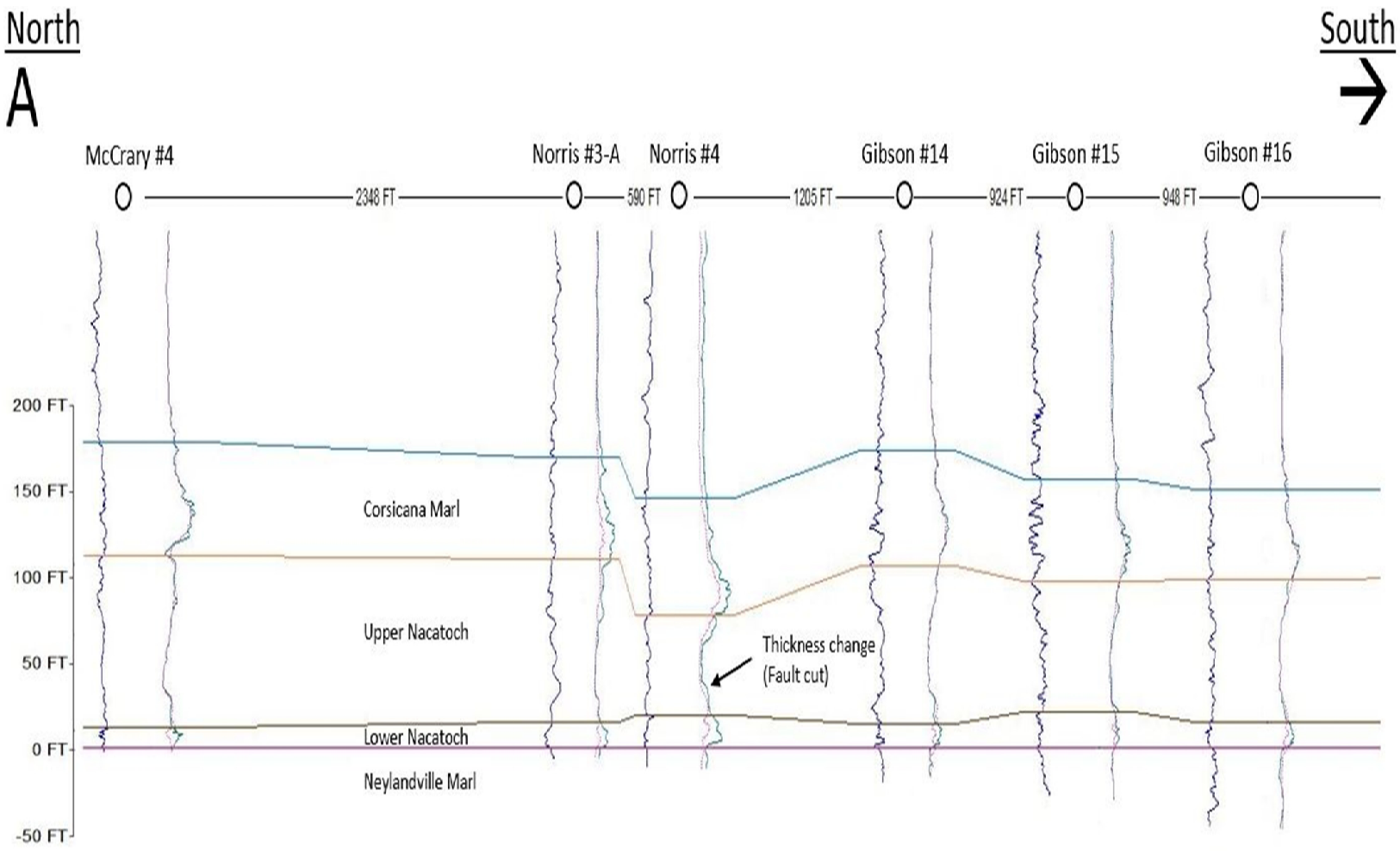

Figure 11A. North half of strike oriented cross-section (A to A'). Neylandville Marl is datum. The lower Nacatoch has thickness variation north to south. See figure 7 for map orientation.

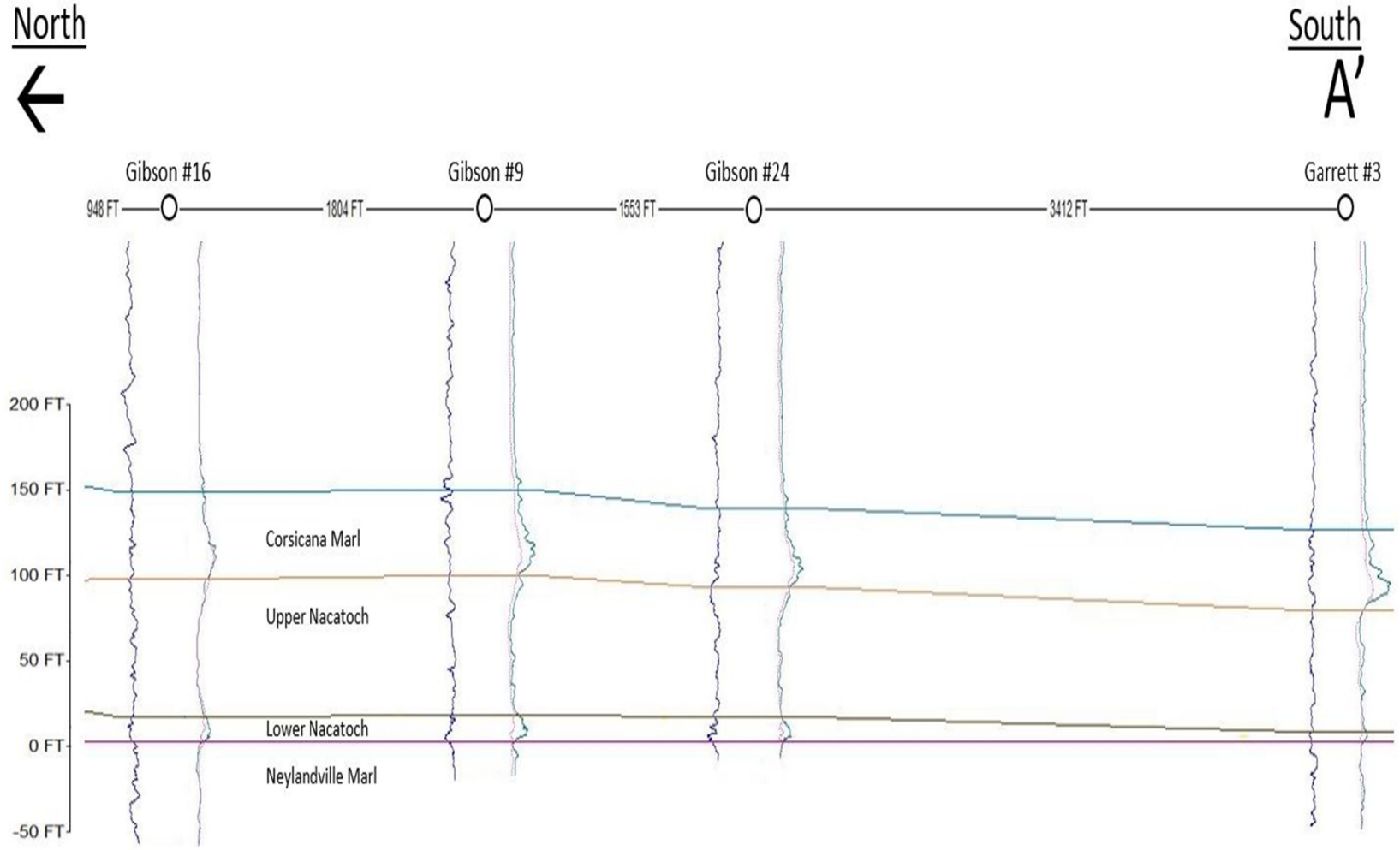

Figure 11B. South half of strike oriented cross-section (A to A'). Neylandville Marl is datum. The lower Nacatoch has thickness variation north to south. See figure 7 for map orientation.

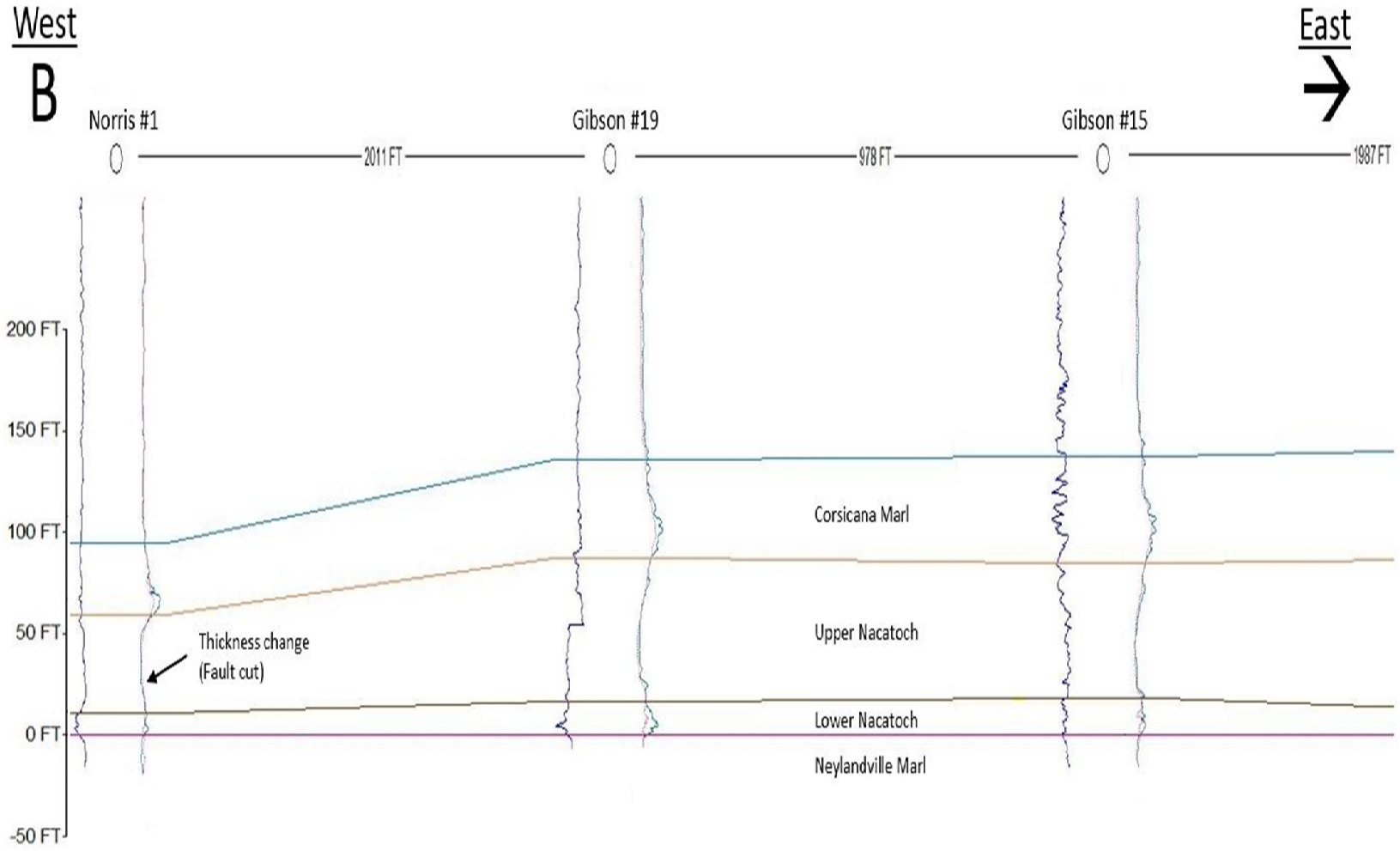

Figure 12A. West half of dip oriented cross-section (B to B'). Neylandville Marl is datum. The lower Nacatoch pinches out to the east and thins to the west. See figure 7 for map orientation.

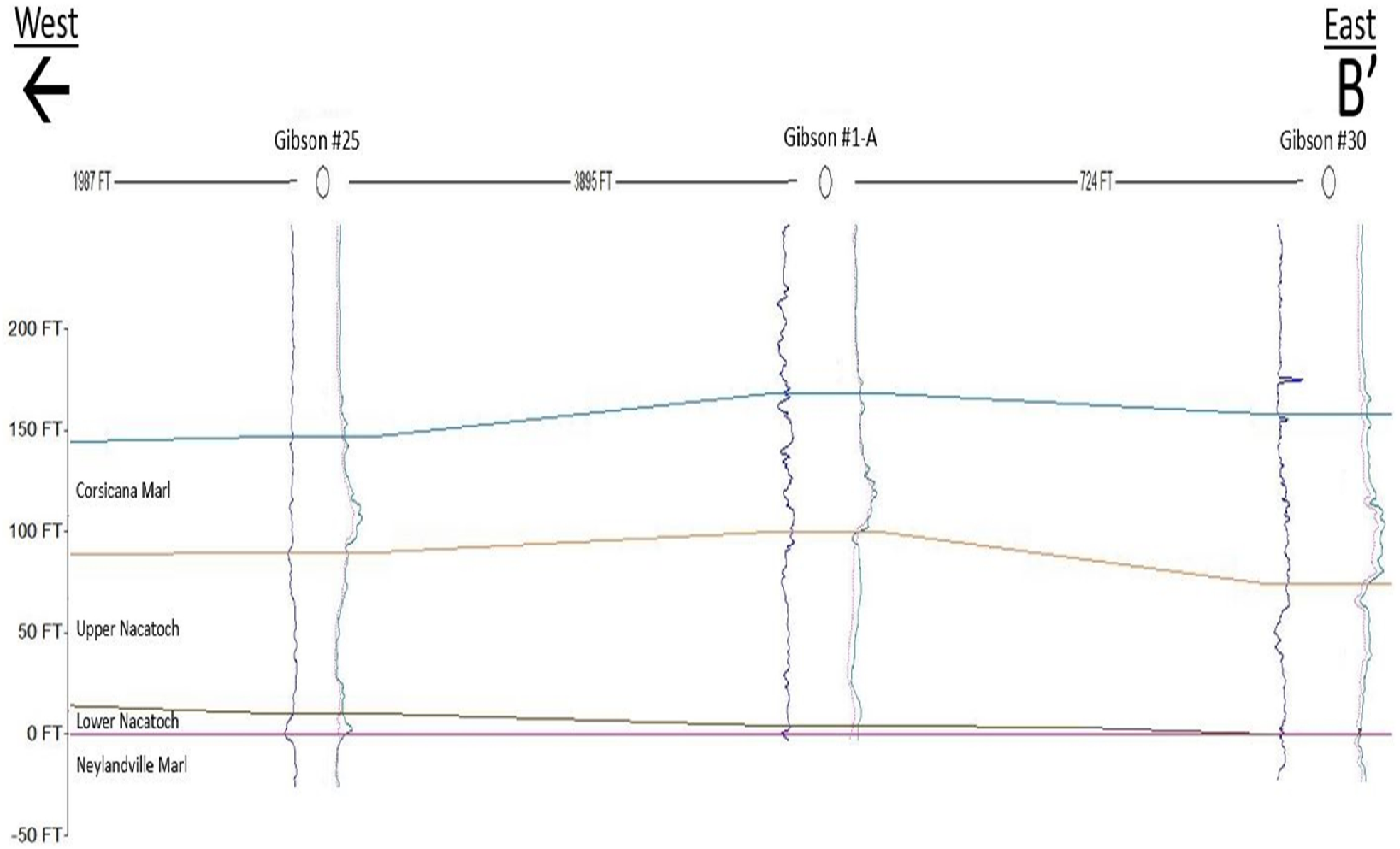

Figure 12B. East half of dip oriented cross-section (B to B'). Neylandville Marl is datum. The lower Nacatoch pinches out to the east and thins to the west. See figure 7 for map orientation.

a reciprocal manner relative to the underlying lower Nacatoch. The lower Nacatoch interval is present throughout the Calvert field, varying from 6 to 20 ft thick but was not observed outside the study area. The lower Nacatoch thins to the north and south (Figure 11 A&B) and pinches out to the east and thins to the west (Figure 12 A&B). Well log resolution was not sufficient to trace individual beds within the lower Nacatoch interval. If sedimentation rate was consistent throughout the deposition of the upper Nacatoch, thinning over the thicker and more sand rich areas of the lower Nacatoch, it suggests that the lower Nacatoch sands were topographic highs.

The main faults that bound the study area are antithetic to the Luling-Mexia-Talco Fault Zone and can be clearly seen as offsets on the west and east boundaries of the study area (Figure 13a and 13b). The larger fault of the two is on the west boundary with a displacement of approximately 181 ft (55 m). The second major fault is on the east boundary and has a displacement of approximately 150 ft (46 m). The study area is structurally complex and based on the lack of growth features across faults, the majority of movement most likely occurred after the deposition of the lower Nacatoch interval. A total of nine wells show normal faults cross-cutting the thickness of the upper Nacatoch, resulting in a loss of approximately half the thickness of the unit.

III.1.2.c Cross-Section Interpretation

The lower Nacatoch thins out to the north and south (Figure 11) and pinches out entirely from the west to the east (Figure 12). The upper Nacatoch and the Corsicana Marl both thicken basinwards to the east and thin towards the west. This suggests that the basin was deeper towards the east and shallower towards the west.

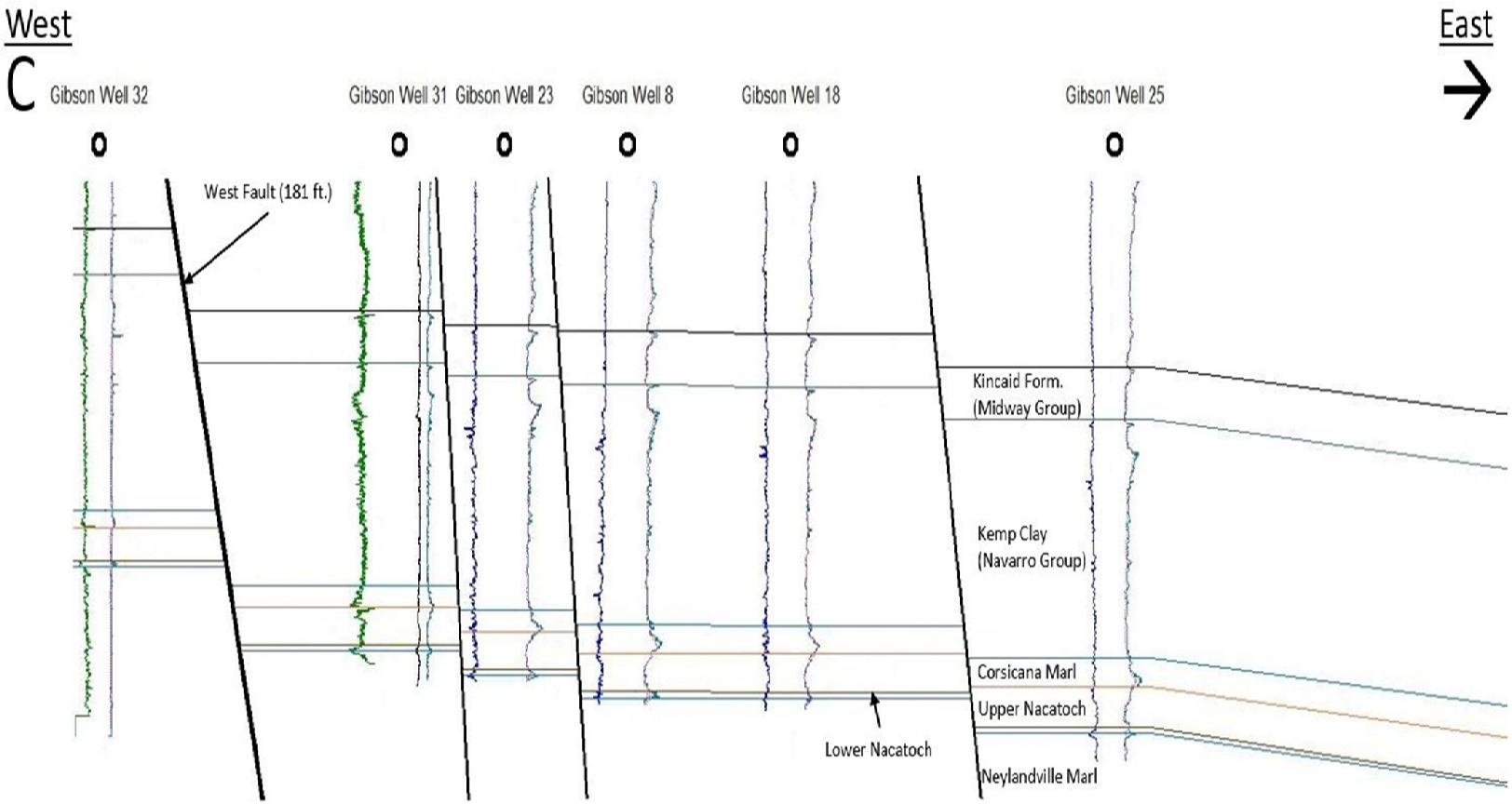

Figure 13A. Dip oriented cross-section of the west half of the study area (C to C'). Displays the structural relief of the synthetic faults in along dip taken perpendicular to the faults. Log curves are as follows: Green (GR), black and dark blue (SP), teal (Shallow RS), pink (Deep RS). See figure 7 for map orientation.

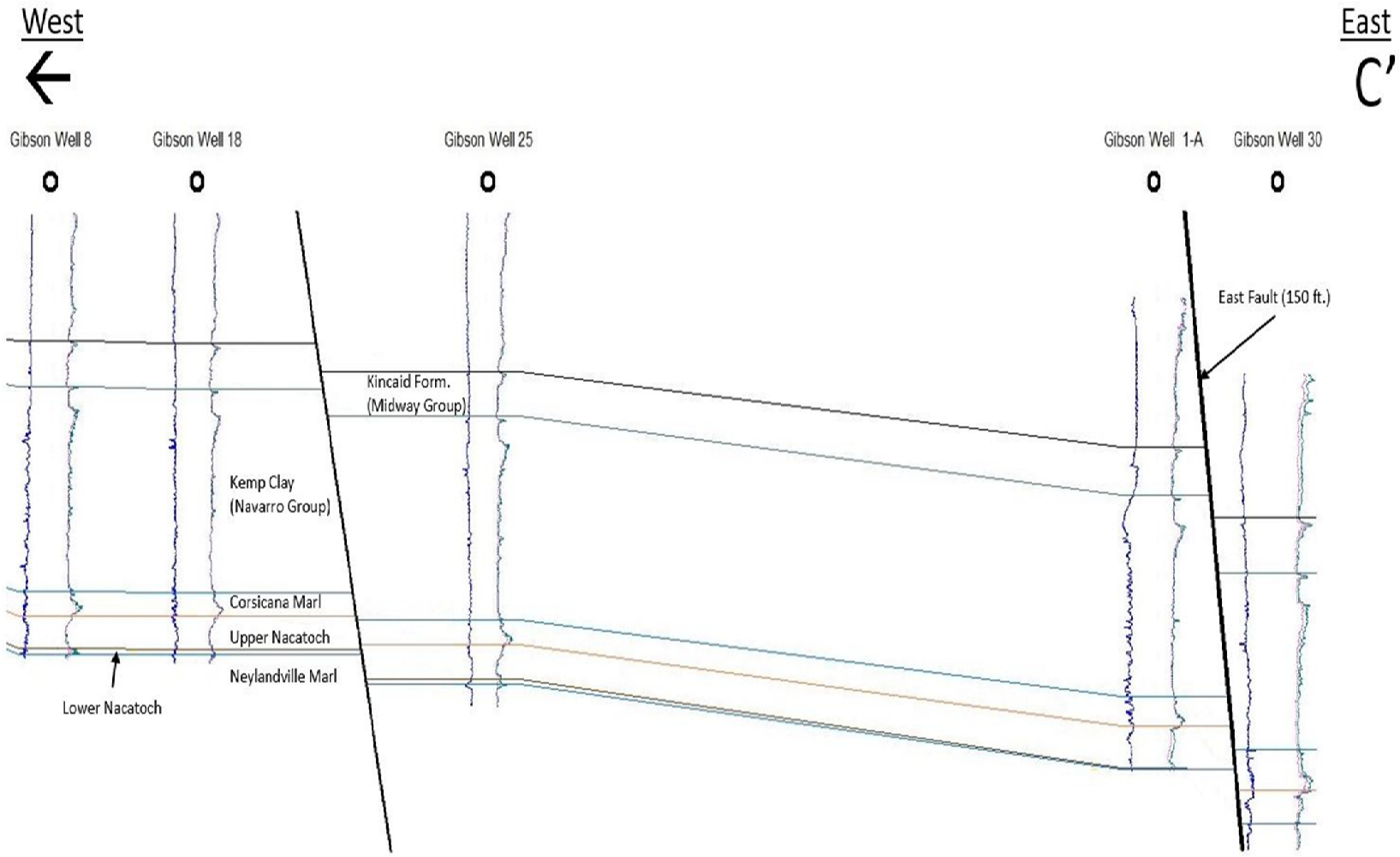

Figure 13B. Dip oriented cross-section of the east half of the study area (C to C'). Displays the structural relief of the synthetic faults in along dip taken perpendicular to the faults. Log curves are as follows: Green (GR), black and dark blue (SP), teal (Shallow RS), pink (Deep RS). See figure 7 for map orientation.

III.1.3 Maps

Maps in this study were used to identify depositional geometries in the study area. This information constrains the lateral extent and frequency of the correlated layers in the interval and helps interpret the paleodepositional environment.

III.1.3.a Map Generation

Isopach, net sand, net-to-gross, and fault maps were created for the upper and lower Nacatoch interval. Although NeuraSection software auto-contouring was originally used to generate maps, these were subsequently re-interpreted by hand because the automated contouring algorithm created odd geometries and many contour closures. The maps were contoured in intervals of 2, 3, 4 and 5 feet in order to get a full perspective of important features.

Structural maps were also created in the software package for the study area. Faults were inferred if the top of the Corsicana Marl surface exceeded 2.5° degrees of dip between wells. The Corsicana Marl was used to compare dip changes throughout the study area between wells because of its extensive and conformable upper stratigraphic surface. There were no observable thickness changes of the lithological units within the study area on either side of the faults.

III.1.3.b Map Results

Isopach, net sand, and net-to-gross maps all illustrate elongated contours that are oriented northwest to southeast. Based on the lower Nacatoch isopach map and net sand map (Figures 14 and 15) the spacing between each elongate feature is approximately 900 ft to 1600 ft (0.2-0.5 km) and they are 1300 ft to 4500 ft (390-1400 m) long. Thickness

differences of these features are approximately 3 ft to 9 ft (1-3 m). The net sand map of the lower Nacatoch depicts larger sand quantities located in the thicker sections of the lower Nacatoch isopach map (Figure 15). The net-to-gross map shows larger percentages of sand located in thicker sections as well (Figure 16). The isopach map of the upper Nacatoch shows a reciprocating thinning and thickening compared to the lower Nacatoch (Figure 17). Furthermore, the upper Nacatoch thickens in the areas of lower sand values and thins in areas of higher sand values of the lower Nacatoch. The total Nacatoch Formation thickness shows a decrease from 110 ft in the north to 80 ft in the south part of the study area (Figure 18).

III.1.3.c Map Interpretation

The Lower Nacatoch interval is interpreted to represent sand bars on an open marine shelf. The bars are dip elongate and show coincident increase in sand thickness with sand percent. The thinning of both the upper and lower Nacatoch interval is evidence for positive relief of the lower Nacatoch bars. These stratigraphic features and the surrounding sediments pinch out to the east and significantly thin to the west suggesting that they were isolated sand bodies (McGowen and Lopez, 1983).

The orientation of the bar features suggests they are storm generated based on criteria distinguishing offshore tidal sand banks and storm-generated sand ridges (Belderson, 1986). The criteria for storm-generated sand ridges are: 1) angle to coastline up to 60°; 2) sand waves rare to absent; 3) obliquity to main flow up to 60°; 4) height range between 3-12 m; 5) smooth crests; 6) slope angles 2° or less; 7) spacing 0.5 to 7 km; 8) lengths of bar features 20 km or less; and 9) internal structure with possible

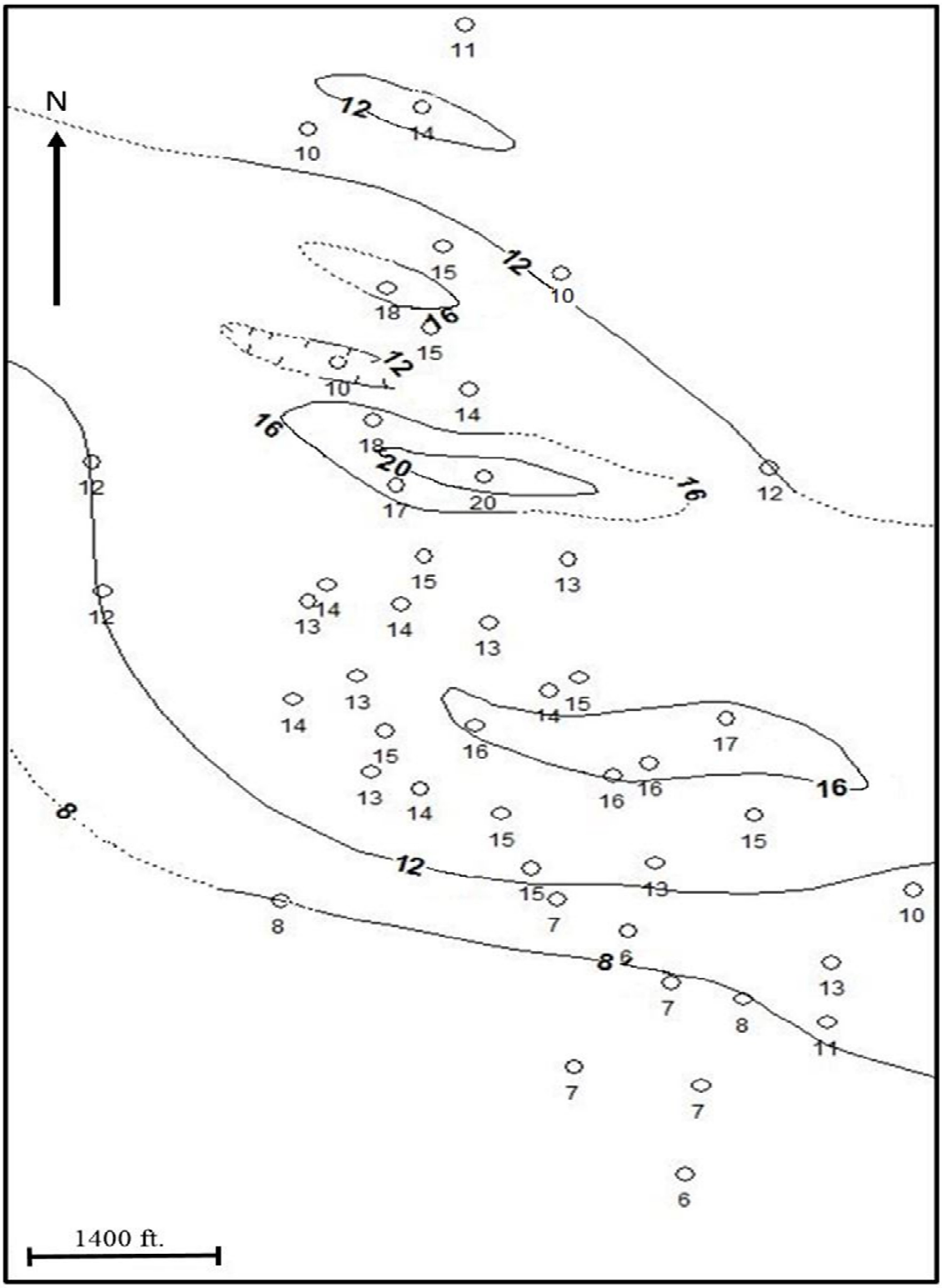

Figure 14. Isopach map of the lower Nacatoch interval.
Contour Interval = 4ft.

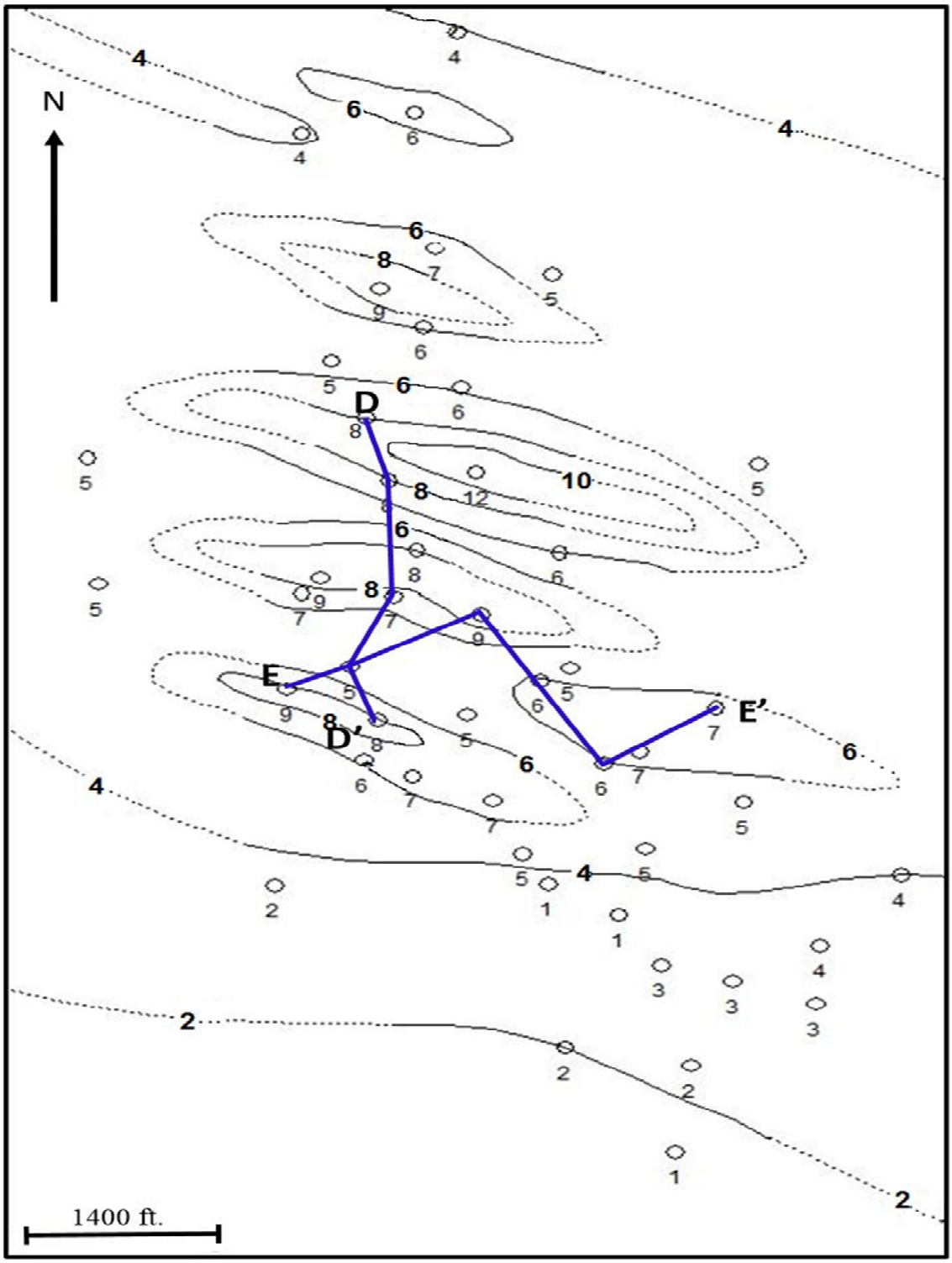

Figure 15. Net sand map of the lower Nacatoch interval. Cross-sections from cores shown in Figure 21.
Contour Interval = 2ft

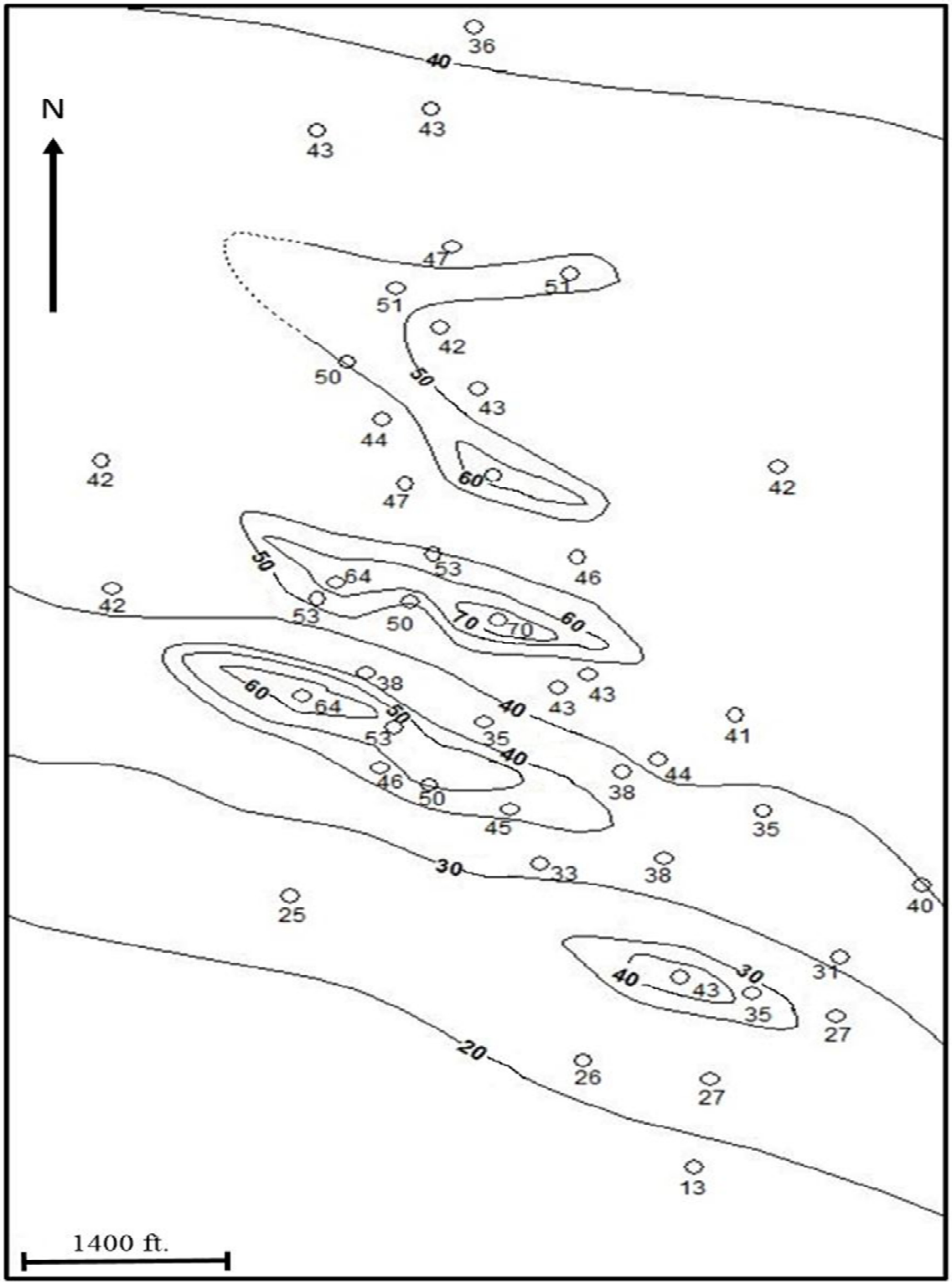

Figure 16. Net-to-gross map of the lower Nacatoch interval.
Contour Interval = 10%

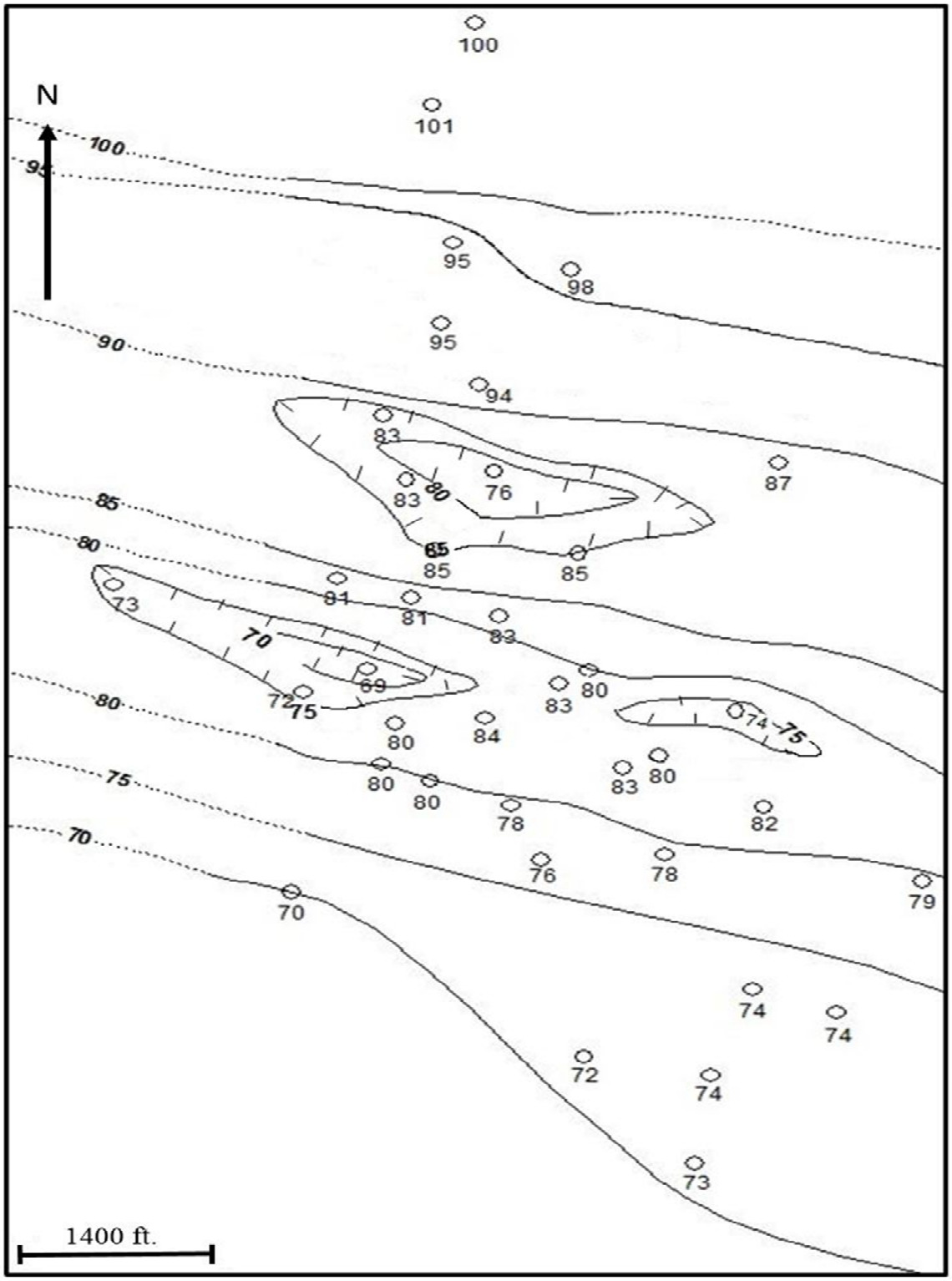

Figure 17. Isopach map of the upper Nacatoch interval.
Contour Interval = 5ft

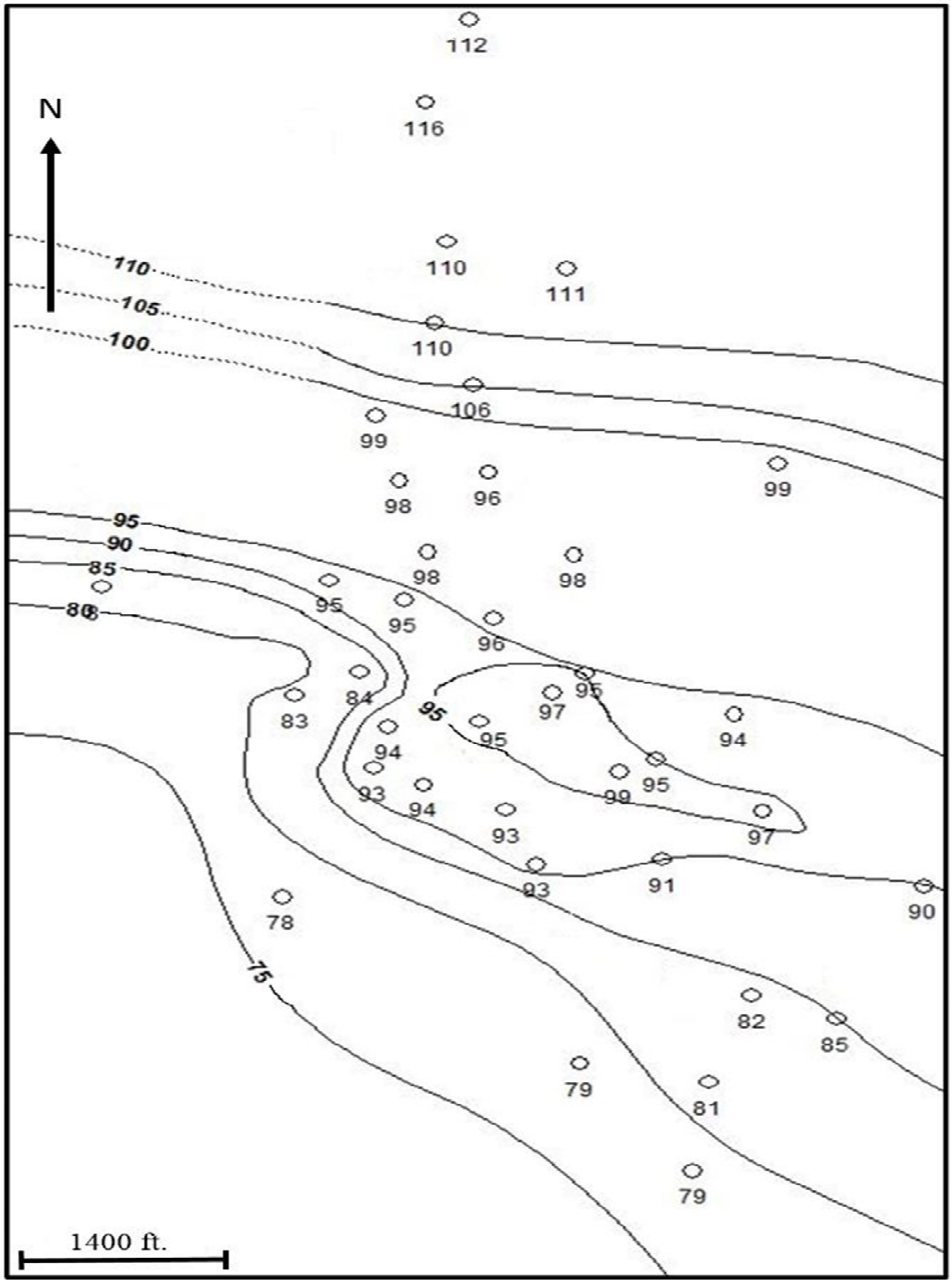

Figure 18. Isopach map of the total Nacatoch Formation.
Contour Interval =5ft

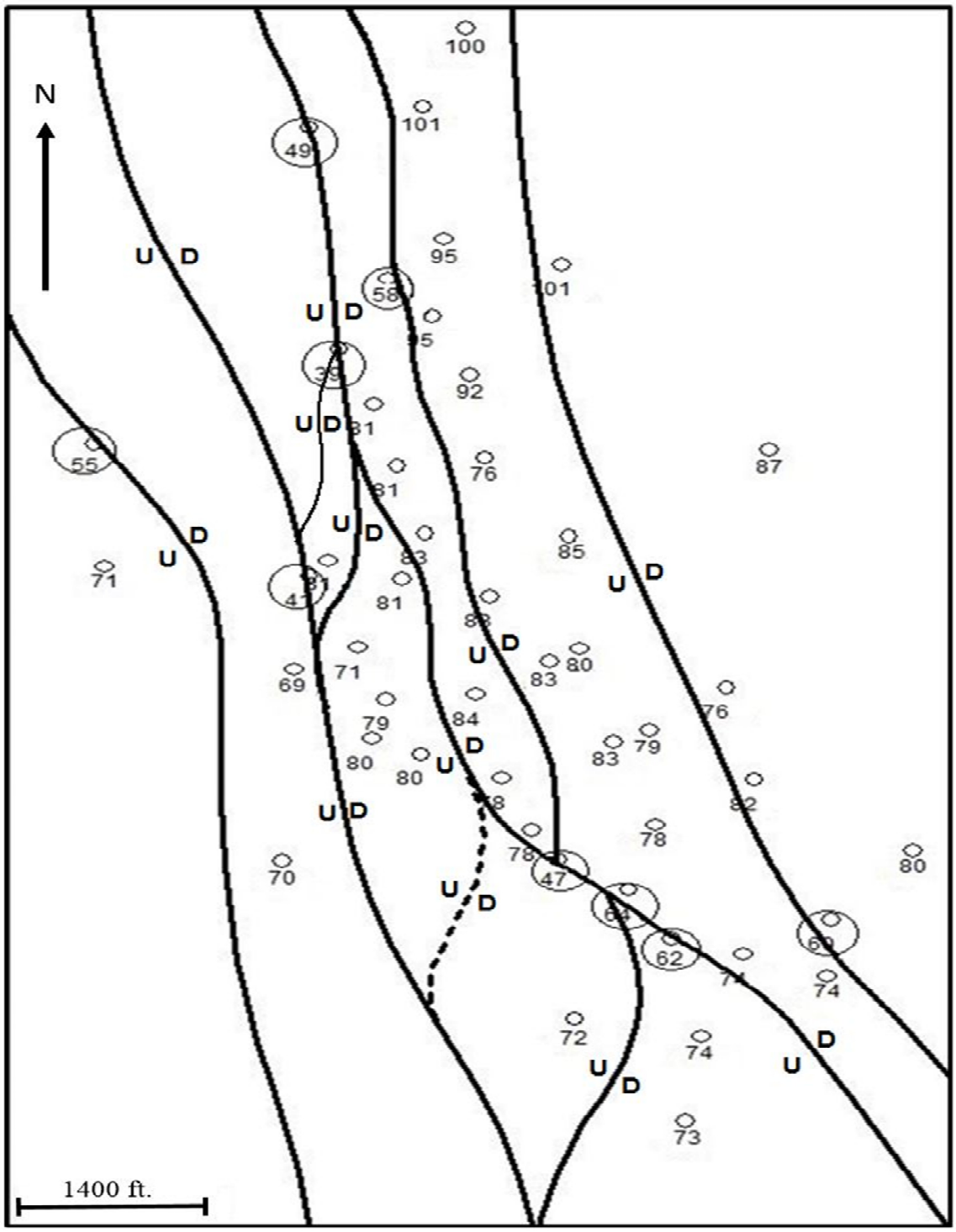

Figure 19. Fault map with upper Nacatoch thicknesses. Faults determined by dip > 2.5° degrees on the top of the Corsicana Marl between 2 or more wells. Circled wells represent where faults were cut (missing thicknesses in the upper Nacatoch interval).

hummocky cross-stratification. The criteria for offshore tidal sand banks are: 1) angle is primarily related to peak tidal current direction; 2) sand waves are abundant and semipermanent; 3) obliquity to main flow is 0°-20°, but generally 7°-15°; 4) height is up to 43 m; 5) sharp crests except where close to sea surface; 6) slope angles are 6° or less; 7) spacing is 2-30 km; 8) length is up to 70 km; and 9) internal structure has pervasive cross stratification. The features of the lower Nacatoch interval are not consistent with the traits of tidally influences sand banks.

The study area is bound by two major faults antithetic to Luling-Mexia-Talco Fault Zone. Figure 19 shows a map view of the faults in the Calvert field and also indicates wells in which the upper Nacatoch was cut by faults. With respect to any relationship between depositional and structural deformation, the upper Nacatoch and Corsicana Marl do not show variations in thickness within individual fault blocks, but rather display basinward thickening towards the east. Faulting must have occurred after rather than during the deposition of the lower Nacatoch, upper Nacatoch and Corsicana Marl, otherwise thickness would be greater on downthrown sides of faults due to increase in accommodation and preservation of sediments.

III.2 DRILL CUTTINGS

Drill cuttings were used from the base of the Nacatoch Formation to the top of the Corsicana Marl. Drill cuttings assist identifying facies, vertical grain size distribution, faunal associations, minerals, and help determine transgressive vs. regressive patterns in an overall stratigraphic context.

III.2.1 Drill Cutting Collection

Drill Cuttings were collected from the Gibson #31 well in early 2013. Samples were collected every 30 ft from the top of the Kincaid Formation of the Midway Group to the top of the Kemp Clay of the Navarro Group. The sample collection interval decreased from the top of the Kemp Clay to the top of the Neylandville Marl to every 10 ft with each sample collected 5 ft after a drill string connection, in the middle of connection, and 5 ft before a new connection. Sampling 5 ft before and after each connection ensured that the samples being collected were from the suspension of actual formation sediments during circulation of the mud up the wellbore.

III.2.2 Drill Cutting Processing

Drill cuttings from the interval from the base of the lower Nacatoch Formation to the upper surface of the Corsicana Marl from the Gibson # 31 were cleaned over a 63 micron (80 mesh) sieve and dried for approximately 12 hours at 150 degrees Fahrenheit. Samples were labeled, recorded and evaluated using a binocular microscope.

III.2.3 Drill Cutting Results

Three different facies were described and identified from the base of the lower Nacatoch interval, through the upper Nacatoch interval to the top of the Corsicana Marl (Figure 20). The different facies identified from cuttings of the Gibson #31 were matched to the well log based on gamma ray (GR), spontaneous potential (SP), resistivity (RS), photoelectric factor (PEF), bulk density (RhoB), neutron porosity (NP) and density porosity (DP) log responses (Figure 8). The *sandstone facies*, which

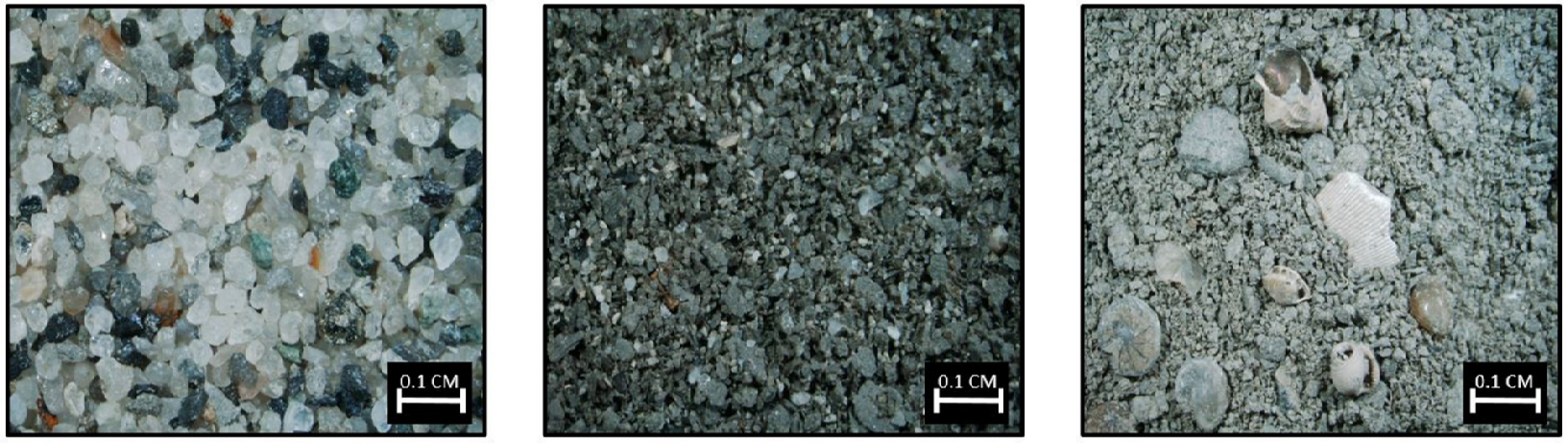

A. Sandstone Facies **B.** Siltstone Facies **C.** Marl Facies

Figure 20. Facies based on drill cuttings. **(A)** Sandstone facies (Lower Nacatoch Formation). **(B)** Siltstone facies (Upper Nacatoch Formation). **(C)** Marl facies (Corsicana Marl). Facies descriptions are in Appendix B.

corresponds to the lower Nacatoch interval, is gray, medium to coarse grained and moderately sorted. It consists of quartz grains, glauconite, pyrite, muscovite, and black fragments that include inoceramids, echinoid spines, organic plant matter and crystallized hydrocarbons. The *siltstone facies*, which corresponds to the upper Nacatoch interval, is medium to dark gray with ostracods, gastropods, *Lenticulina* foraminifera and shell fragments. In some places, the siltstone facies has very hard limestone and shale fragments along with crystallized hydrocarbon and sparse amounts of pyrite inclusions. The *marl facies*, which corresponds to the Corsicana Marl, is light gray to white marl, very fine grained, sub-rounded to rounded with poor cementation that is highly calcitic. It has inoceramids, mollusks, *Lenticulina* foraminifera and sparse plant fragments.

III.2.4 Drill Cutting Interpretation

The *sandstone facies* is interpreted as a marine shelf sand deposit. The broken shell fragments and plant matter suggests reworking within the sand and could indicate that the fossils are allochthonous as suggested by Stephenson (1941). Glauconite found in the sandstone facies ranges from dark green to very light green. Stonecipher (1999) suggests that during transgression, sediments from older lowstand deposits (landward) can be reworked and incorporate different types (seen in both color and shape) of glauconite in transgressive deposits (seaward). The different types of glauconite deposited in the isolated lower Nacatoch interval are interpreted to indicate up-dip sediment reworking by storm processes and/or transgressive ravinement processes.

The *siltstone facies* is interpreted as a middle to outer shelf deposit below storm-weather wave base. The presence of shell fragments and large quantities of *Lenticulina* along with ostracods and gastropods suggest a diverse benthic biota and is considered to represent a deeper shelf depositional environment.

The *marl facies* is interpreted and characterized as an outer shelf (distal) deposit based on: 1) the increasing thickness basinwards, 2) the fine grained carbonate nature of the sediment, and 3) the extensive distribution of the unit as suggested by McGowen and Lopez (1983). This facies is the deepest of the three identified and the vertical succession of facies indicates a deepening up section.

III.3 CORE DATA

Core data was used to understand the internal structure of the lower Nacatoch Formation. Core data descriptions narrowed possible of depositional processes that were responsible for the lower Nacatoch interval.

III.3.1 Core Collection

A private log library maintained by P.K Reiter at Warrior Resources LLC had 22 previous core descriptions that were part of the exploration project in the study area during the 1940s and were utilized in this study to supplement well log interpretations. The original core descriptions were analyzed and tied to new wells using the top of the Neylandville Marl as a datum, because this shale was reported at the bottom of all the old core descriptions (Figure 21).

III.3.2 Core Results

Five lithologies were described in cores of the lower Nacatoch. The *black shale* encases the lower Nacatoch interval stratigraphically and corresponds to the siltstone facies of the upper Nacatoch interval and Neylandville Marl identified in drill cuttings. The *sandstone,* which is described as clean sand occurring in 3 in to 3 ft beds, corresponds to the sandstone facies identified in drill cuttings from the lower Nacatoch interval. The core indicates the presence of pebble layers in some sandstone beds. The *brown shale* forms 3 in to 3 ft thick interbeds with the *sandstones* in the lower Nacatoch interval. The *interbedded sand and shale* lithology forms beds < 3 in thick in the lower Nacatoch. Finally, the *sandy shale* is intermittent throughout the lower Nacatoch interval (Figure 21).

III.3.3 Core Interpretation

Reworked sediment, medium to coarse grained sand, along with interbedded sands and shales described in core are characteristics of both storm and tide dominated shallow siliciclastic coastal processes (Nichols, 2009; Elliot, 1978). Correlations between the cores, grain size distribution, well log curves, and the glauconite found in the cuttings (Figure 22) compared to the typical shelf facies (Figure 23), indicate that the environment was below fairweather wave base, storm-dominated and deposited on the middle to outer shelf and are easily preserved (Johnson, 1978).

The *black shale* encases the lower Nacatoch interval and is interpreted as offshore, outer shelf marine deposits (Figure 22). The *sandstone* and *brown shales* in the lower Nacatoch interval are interpreted as storm event cycles formed by large or

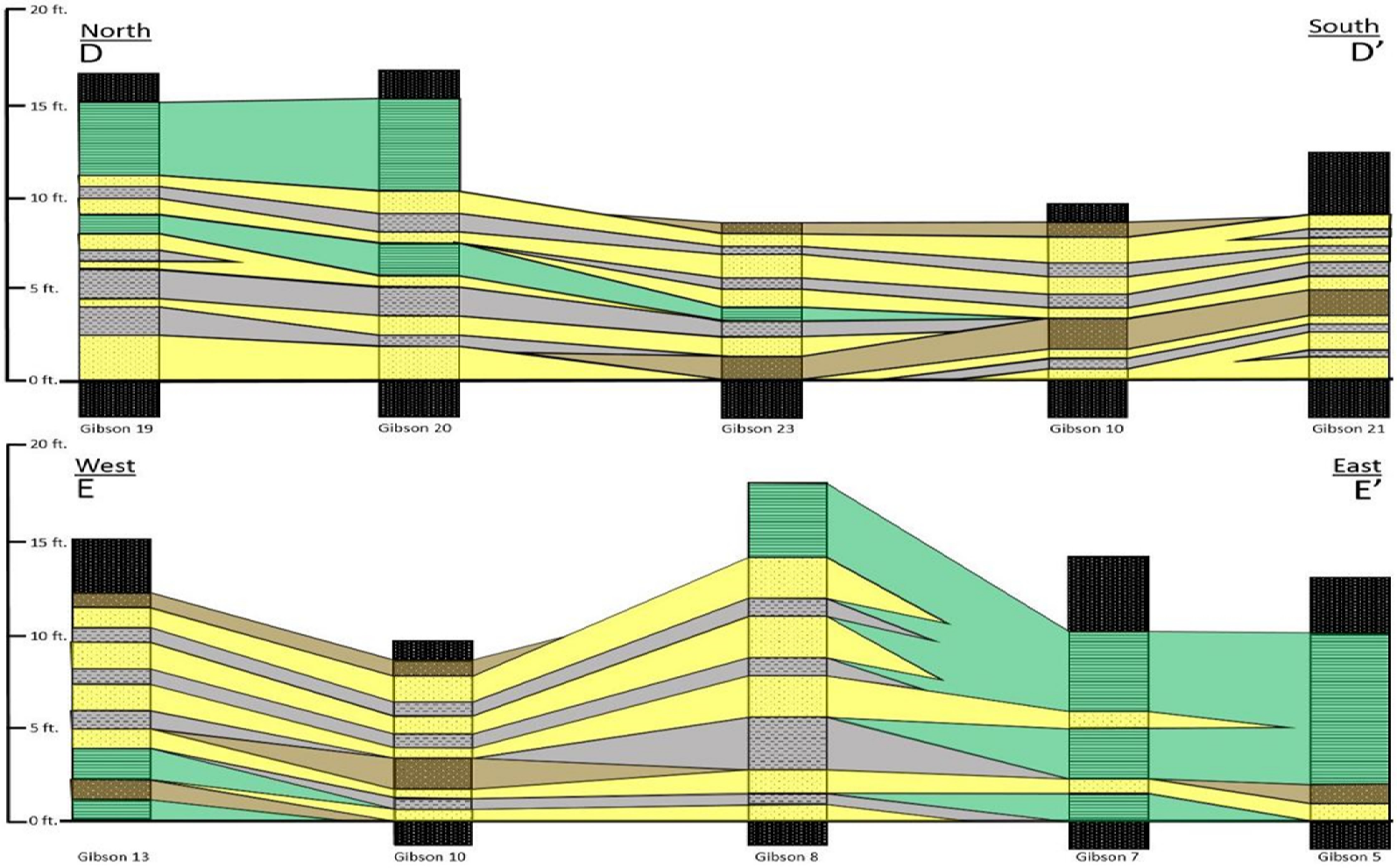

Figure 21. Core cross-sections in the lower Nacatoch interval. **(D to D')** Cross-section along strike from north to south. **(E to E')** Cross-section along dip from west to east. Each cross-section depicts the interbedded sand and shales (Green), sands (Yellow), shales (Gray), sandy shales (Brown) and Black Shales (Black). See Figure 15 for orientation of core cross-sections.

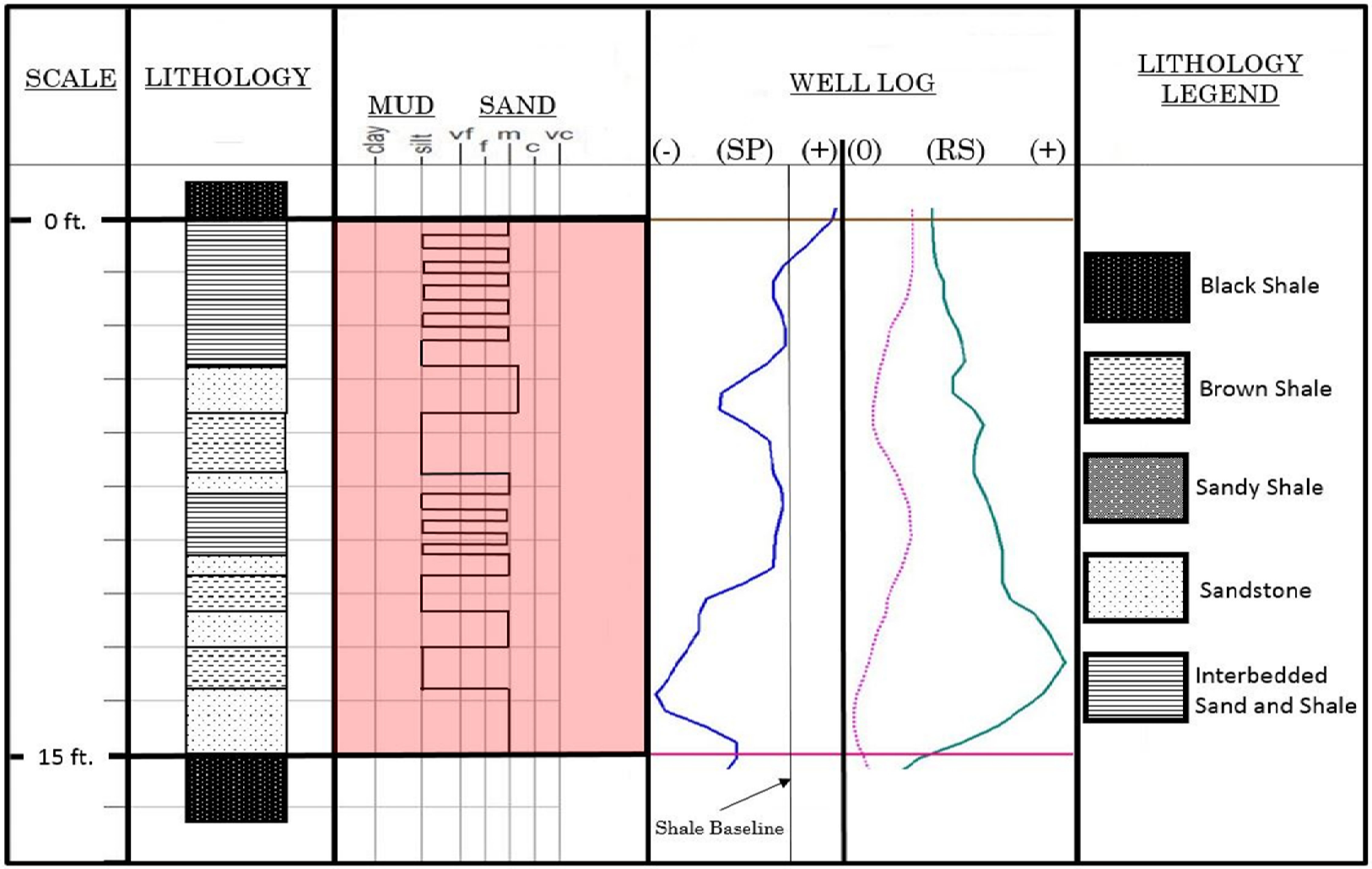

Figure 22. Study area stratigraphic comparison. Correlation in depth between core lithology, grain size and well log of the Gibson #20 Well. The well log curves from left to right are: Spontaneous potential (SP), Deep (RS), and Shallow (RS).

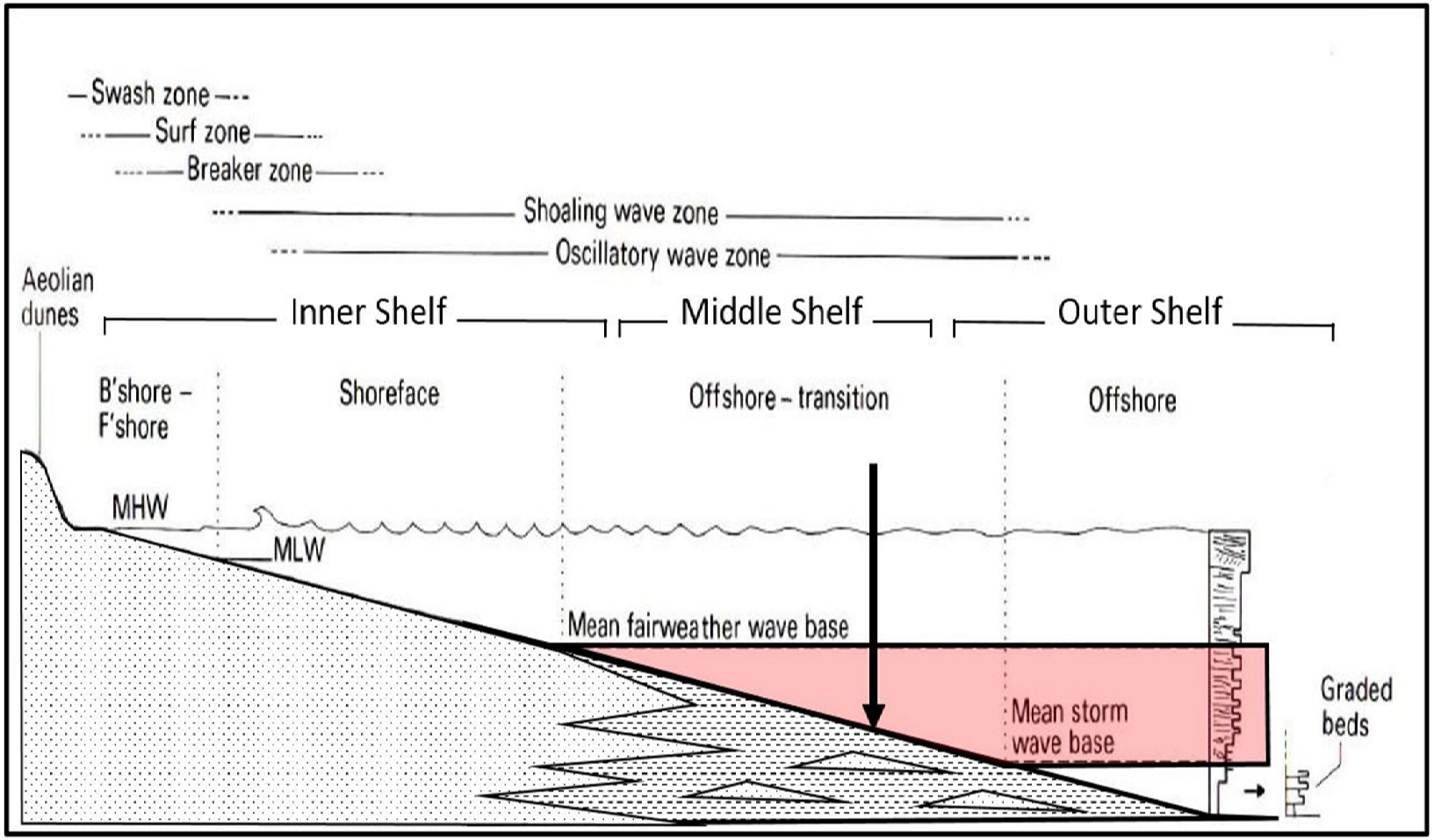

Figure 23. Facies stratigraphic comparison. Beach environments and facies associations help identify storm-dominated deposition as offshore-transition zone (Middle shelf). The lower Nacatoch interval laminated beds were deposited below fairweather wave base with an approximate shelf position indicated by the arrow (Modified from Elliot, 1978).

proximal storm events. The pebbles found in some of the sandstones could represent lag deposits (Plint, 2010; Clifton 2006). The *interbedded sand and shale* consist of thinly interbedded sand and shale laminations interpreted as the product of small storms or distal storm events. The *sandy shale* is interpreted to represent fair weather deposition between storms events.

III.4 SUMMARY OF RESULTS

The Nacatoch Formation was divided into 2 parts (upper and lower intervals) based on well logs, drill cuttings and core descriptions. The interval from the base of the Nacatoch Formation to the top of the Corsicana Marl is a fining upwards sequence seen in well logs. The fining upwards sequence was described and confirmed by the Gibson # 31 drill cuttings analysis. The internal stratigraphy of the lower Nacatoch interval is interbedded sand and shale of variable thicknesses and dimensions. Well logs in conjunction with the core descriptions and drill cuttings indicate the succession is overall deepening. Different types of fossils and glauconite described indicate marine origin, reworked sediment and an approximate location on the middle to outer shelf. The cross-sections created in the study area from well logs suggest that the lower Nacatoch interval is an isolated sand body that thins to the north, south and west and pinches out to the east. Stratigraphically, the geometries in both the maps and the cross-sections show that the variable thickness of the lower Nacatoch interval represents elongate bars oriented northwest to southeast. All the varied data concur that the study area represents a middle to outer shelf storm-dominated deposit.

IV. DISCUSSION

IV.1 INTERPRETED PALEODEPOSITIONAL ENVIRONMENT

The lower Nacatoch is an isolated shelf sand body. Three requirements need to be met to create shelf ridges or bars: 1) sufficient amounts of sand; 2) currents capable of moving sand; and 3) pre-existing irregularities on the basal surface. Snedden and Bergmann (1999) identified the three types of ridge/bar and their general requirements.

The first type is a Shelf Sand Ridge that onlap underlying lithologies, are coarse grained with high permeability and high anisotropy, and form on or close to paleo-highs, possibly from old ebb tidal deltas. They are associated with transgressive systems tracts and orientation is shore oblique to shore parallel.

The second type is an Incised Lowstand Shoreface, which display toplap and erosional surfaces at top and bottom. Vertical and horizontal grain size is variable, internal surfaces dip seaward, and large-scale bars are oriented shore parallel.

Finally, the third type is an Incised Valley Fill, which are characterized by toplap and truncation onto base lithologies. Grain sizes and sand percent is variable, possibly filling paleo-lows. Incised Valley Fills display clinoforms within valleys and are oriented shore parallel or shore normal.

The Shelf Sand Ridge is most likely to be the type of sand ridge associated with the lower Nacatoch interval because it is transgressive, represents a paleohigh and is coarse grained. Both the Incised Lowstand Shoreface and the Incised Valley Fill are associated with Lowstand System Tracts and have parameters that do not match the lower Nacatoch interval (Snedden and Dalrymple, 1999).

Specific observations diagnosing deposition of the lower Nacatoch interval in a shallow marine environment including the presence of benthic foraminifera, marine macrofossils, and glauconite. Additional observations of the bar forms also helped diagnose depositional environment (tidal vs. non-tidal bars) such as length, width, thickness, orientation, and grain sizes.

The lower Nacatoch interval in the study area represents an isolated sandstone body with closely spaced, low relief, bar forms of relatively short length, oriented 60° or more to paleo-shoreline and composed of medium-grained sands interbedded and interlaminated with shales, incorporating broken shell fragments, woody material, pyrite and glauconite. There is no evidence that the lower Nacatoch sands fill an incised low, and the unit does not display strong evidence of tidal deposition or onlap onto an incision surface truncating underlying units.

Logs and cores show no evidence for truncation associated with a ravinement surface at the top of the lower Nacatoch, as expected in the case of an incised low stand shoreface. The transgressive succession, evidence for deposition influenced by storms as described by Clifton (2006), and shore oblique orientation strongly suggest that the lower Nacatoch interval represents isolated shelf sand ridges deposited below fairweather wave base by storms. Furthermore, preservation of beds in shore proximal deposits during transgression are less likely to survive due to the ravinement process and supports the offshore depositional interpretation of the lower Nacatoch interval (Swift and Parsons, 1999). Figure 24 depicts the location of the study area and Figure 25 illustrates the depositional environment the lower Nacatoch interval represents.

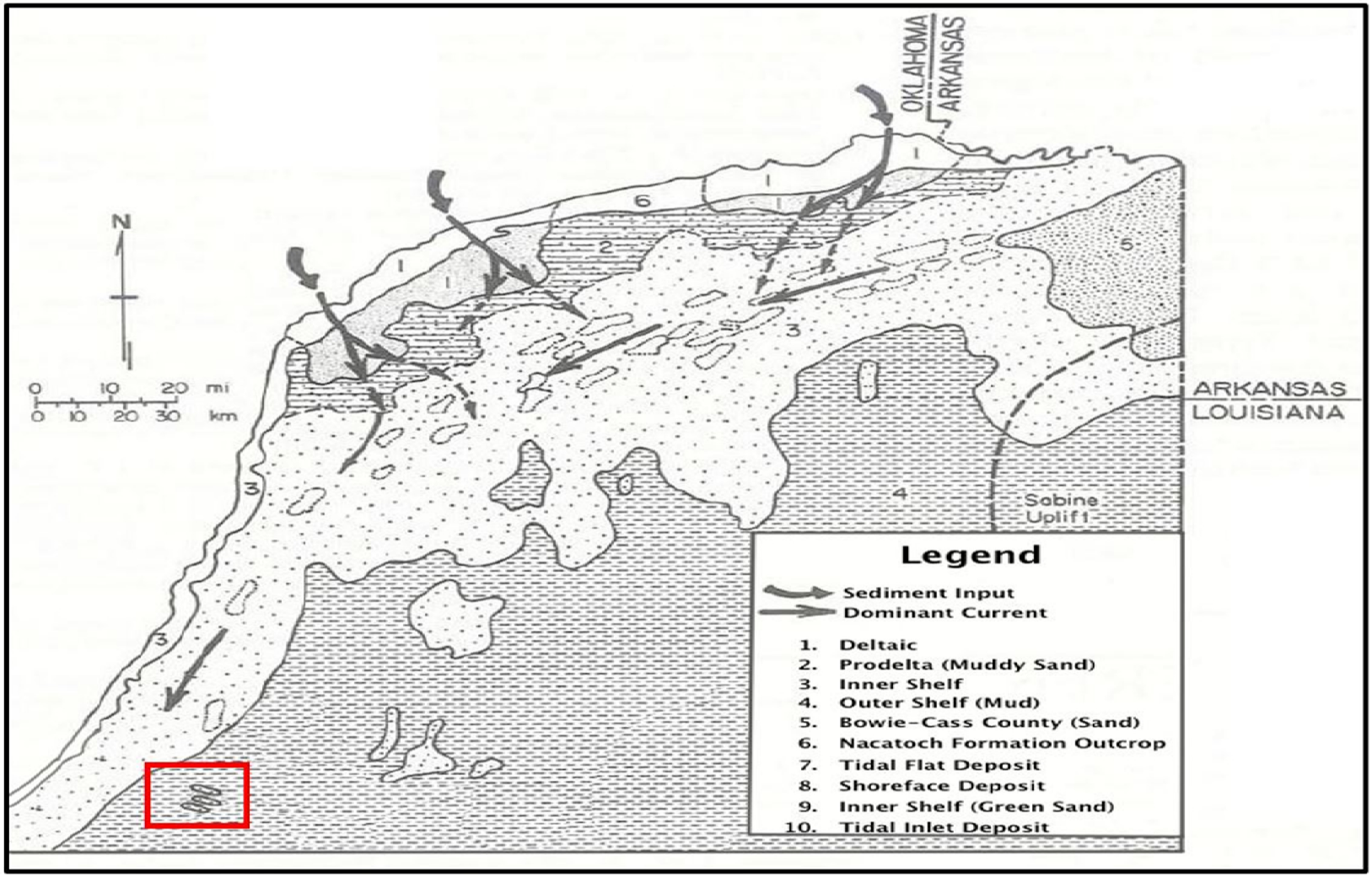

Figure 24. Map of interpreted lower Nacatoch paleodepositional setting. Study area in red box (Modified from McGowen and Lopez, 1983).

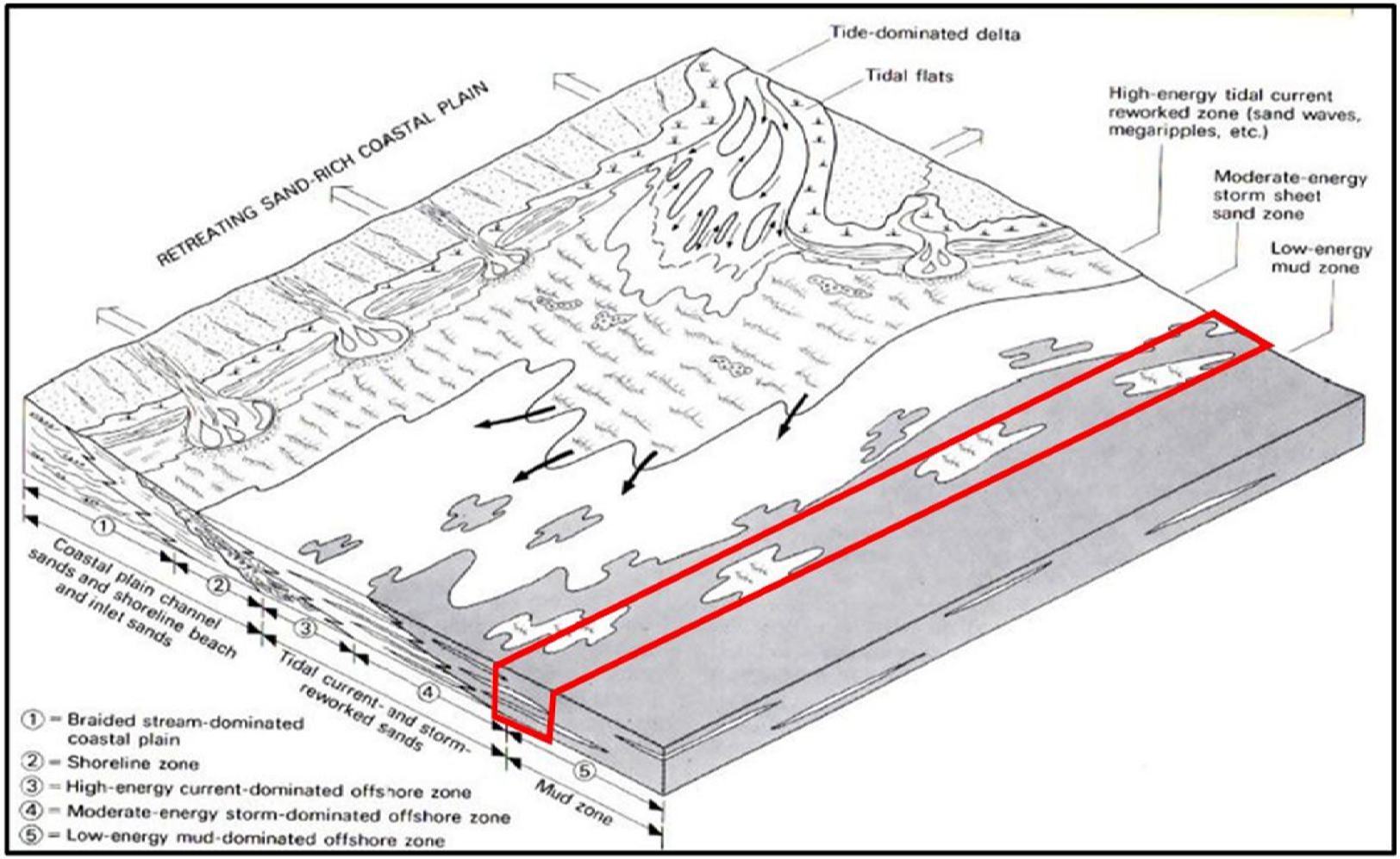

Figure 25. Depositional environments and stratigraphic cutaways, facies and generalized geometries. Red band indicates position of the lower Nacatoch interval in the study area (Modified from Level, 1980).

IV.2 DEPOSITIONAL HISTORY

In the beginning of the Maastrichtian, the Neylandville Marl was deposited overlying an unconformity at the top of the Taylor Group (Figure 26 A). Deposition of the Neylandville Marl was followed by a eustatic sea-level drop (Figure 26 B), allowing the shoreline to advance into the basin and deposit a lowstand shoreface sand body (Figure 26 C). Between the lowstand and early stages of subsequent transgression, the low stand shoreface sand body was reworked by storms and ravinement, providing the source of sand for the lower Nacatoch storm-generated offshore deposit (Figure 26 C), which was deposited as a series of sand and shale couplets, each representing storm events. The lower Nacatoch deposits were deeper than the erosive ravinement, which allowed the sand and shale to be preserved offshore as an isolated sand body.

As sea level continued to rise, the energy level dropped allowing shales to blanket the study area. The orientation of the covered sand bars suggest that the major flow of water during storm events was shore normal. During fairweather, the bars were below wave base and therefore not affected by nearshore current action. The siltstones/black shales of the upper Nacatoch interval represent the increasing rate of eustatic sea-level and the drowning of the lower Nacatoch interval on the middle to outer shelf (Figure 26 D). Finally, at the peak of transgression, the Corsicana Marl was deposited in a deep, outer shelf environment (Figure 26 E).

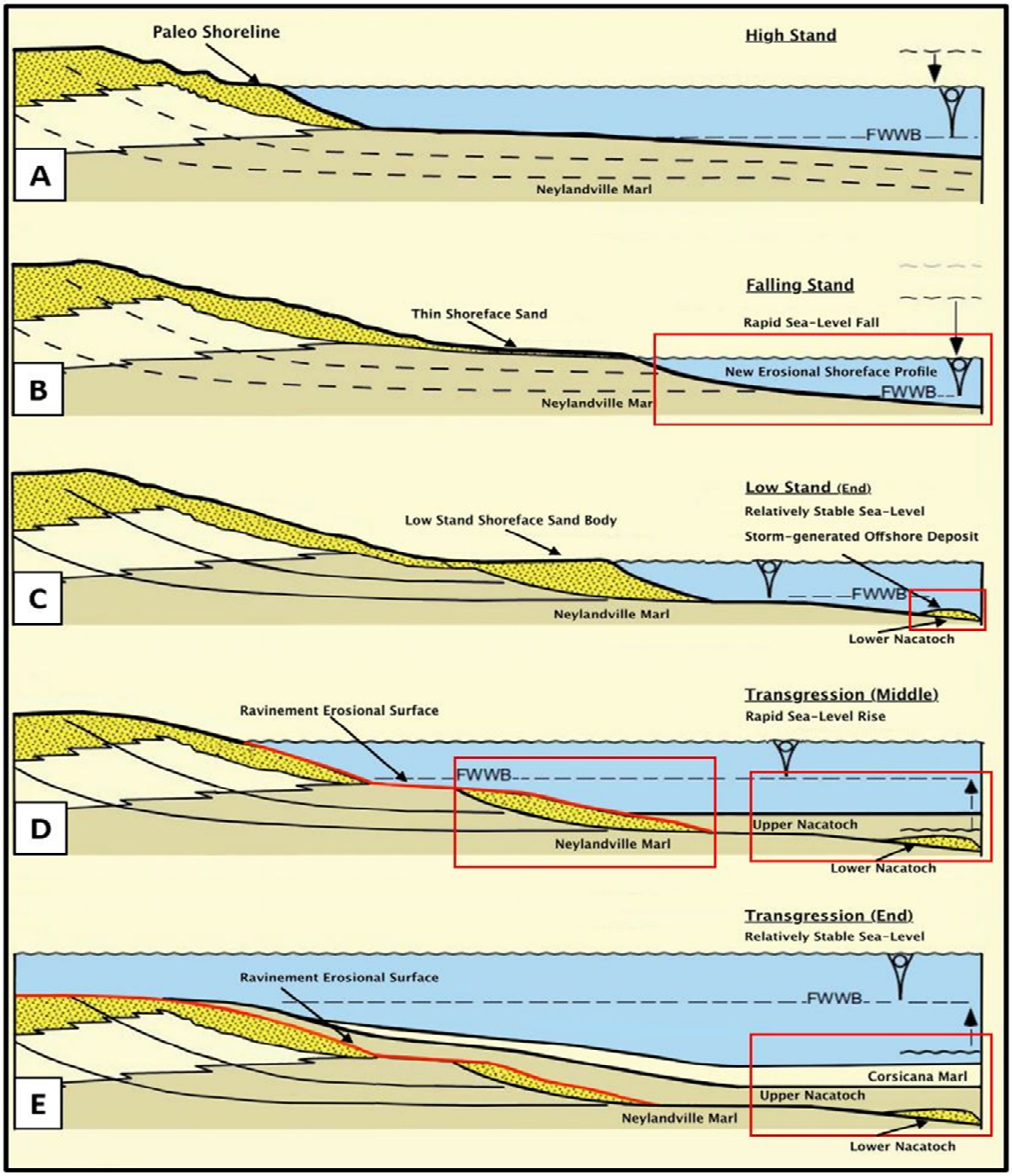

Figure 26. Depositional history of the lower Nacatoch in reference to sequence stratigraphy and shoreline position. **(A)** Post-Neylandville Marl deposition (highstand). **(B)** Rapid sea-level fall during a Falling Stand. **(C)** The lowstand shoreface sand body was deposited first; subsequent storms reworked sediment and deposited bar forms of the lower Nacatoch further out on the shelf. **(D)** Rise of eustatic sea-level. Storms and ravinement reworked the lowstand shoreface sand body until it was nearly destroyed. **(E)** Sea level rise up to peak transgression drowned the shelf and resulted in deposition of the Corsicana Marl (Modified from Clifton, 2006).

V. CONCLUSIONS

Subsurface data identified sedimentary geometries and patterns in the Maastrichtian lower Nacatoch interval in Robertson County, Texas. The well logs and core descriptions allowed mapping of the lower Nacatoch interval separately from the upper Nacatoch interval and characterization of it as an isolated sand body. Depositional and stratigraphic models considered to explain the origin of the lower Nacatoch interval of the Calvert field included incised low stand shoreface, incised valley fills, shelf sand ridges, and storm-generated offshore bars.

The base of the lower Nacatoch to the top of the Corsicana Marl is a fining upwards sequence, recording a eustatic sea-level rise across the Texas coast during the Maastrichtian. New findings in this study include the indication of sand ridge/bars oriented northwest to southeast deposited in a middle to outer shelf environment. Three facies were identified: *sandstones* deposited by storms in offshore settings, *siltstones* deposited in distal offshore settings, and *marl* recording maximum water depth in the study interval.

Five internal lithologies were identified in the lower Nacatoch and were all consistent with storm event beds. Marine shell fragments, microfossils, and glauconite substantiate the inferred marine shelf depositional context. Documentation of storm-deposited shelf bars expands the understanding of the Nacatoch Formation that was previously limited to outcrops of coastal deposits to the north ((McGowen and Lopez, 1983).

The lower Nacatoch interval has bar forms trending northwest to southeast with overall orientation oblique to paleoshoreline. The lower Nacatoch is composed of laminated sand and shale of variable thicknesses and represents a starved, shallow shelf storm-dominated deposit of the Maastrichtian. The depositional architecture of the lower Nacatoch is significant because it effects the vertical and horizontal permeability of an actively produced zone. Exploration and production in this field and its immediate vicinity should take into account the stratigraphic geometries, stratigraphic heterogeneity, structural complexity, and paleogeography before further exploitation can be realized.

REFERENCES

Bain, Richard C., 2004, Exploitation of thin basin-floor fan sandstones, Navarro Formation (Upper Cretaceous), South Texas: Gulf Coast Association of Geological Societies, v. 53, p. 30-37.

Bassiouni, Zaki, 1994, Theory, measurement and interpretation of well logs, Richardson, Texas, Society of Petroleum Engineering, SPE Textbook Series v. 4, 372 p.

Belderson, R.H., 1986, Offshore tidal and non-tidal sand ridges and sheets - differences in morphology and hydrodynamic setting, Canadian Society of Petroleum Geologists, Memoir II, p. 293-301.

Clifton, H. E., 2006, A reexamination of facies models for clastic shorelines, *in* Henry W. Posamentier and Roger G. Walker, eds., Facies models revisited, Tulsa, OK, SEPM (Society of Sedimentary Geologists), Special Publication No. 84, p. 293-337.

Condon, S.M., and T.S. Dyman, 2006, 2003 geologic assessment of undiscovered conventional oil and gas resources in the Upper Cretaceous Navarro and Taylor Groups, Western Gulf Province, Texas: USGS, U.S. Geological Survey Digital Data Series DDS–69–H, Ch. 1-4, p. 1-42

Elliot, T., 1978, Siliciclastic Shorelines, *in* H.G Reading, eds., Sedimentary environments and facies, Oxford, UK, Blackwell Scientific Publication, p. 155-188.

Galloway, William E., 2008, Depositional evolution of the Gulf of Mexico sedimentary basin, Miall, Andrew D.; Hsue, K.J., The sedimentary basins of the United States and Canada, Amsterdam, Netherlands, Elsevier, v. 5, p.505-549

Goldhammer, R.K., and C.A. Johnson, 2001, Middle Jurassic-Upper Cretaceous paleogeographic evolution and sequence - stratigraphic framework of the northwest Gulf of Mexico rim, *in* C. Bartolini, R.T. Buffler, and A. Cantú-Chapa, eds., The western Gulf of Mexico basin: Tectonics, sedimentary basins, and petroleum systems: AAPG Memoir 75, p. 45-81.

Haq, Bilal U., Jan. Hardenbol, and Peter R. Vail, 1988, Mesozoic and Cenozoic chronostratigraphy and cycles of sea-level change: SEPM Special Publication No. 42, Sea-level changes: An integrated approach; p. 96-97.

Johnson, H.G., 1978, Shallow Siliciclastic Seas, *in* H.G Reading, eds., Sedimentary environments and facies, Oxford, UK, Blackwell Scientific Publication, p. 229-258.

Knight, Michael T., John G. McPherson, and Donald F. Reaser, 1984, Deltaic sedimentation in Nacatoch Formation (Late Cretaceous), northeast Texas: AAPG Bulletin, v. 68, p. 496

McCubbin, Donald G., 1981, Barrier-island and strand-plain facies: Sandstone depositional environments, AAPG Special Volume, Volume M 31, p. 247-279.

McGowen, Mary K. and Cynthia M. Lopez, 1983, Depositional systems in the Nacatoch Formation (Upper Cretaceous), north east Texas and southwest Arkansas: Bureau of Economic Geology, Report of Investigations No. 137, p. 1-59.

Miller, Kenneth G.; Kominz, Michelle A.; Browning, James V.; Wright, James D.; Mountain, Gregory S.; Katz, Miriam E.; Sugarman, Peter J.; Cramer, Benjamin S.; Christie-Blick, Nicholas; Pekar, Stephen F., 2005, The Phanerozoic record of global sea-level change: Science, 2005, v. 310 (5752), p.1293-1298

Patterson, Joseph E., Jr., 1983, Exploration potential and variations in shelf plume sandstones, Navarro Group (Maestrichtian), east-central Texas. Master's Thesis, University of Texas, Austin, TX, 101 p.

Patterson, Joseph E., Jr., and Alan J. Scott, 1984, Exploration potential and variations in shelf plume sandstones, Navarro Group (Maestrichtian), east-central Texas: AAPG Bulletin, v. 68 p. 515.

Pirson, Sylvain J., 1981, Geological well log analysis, Houston, TX, Gulf Publishing Company, 377 p.

Plint, E.H., 2010, Wave-and storm-dominated shoreline and shallow marine systems, *in* Noel P. James and Robert W. Dalrypmle, eds., Facies Models 4, St. Johns Newfoundland & Labrador, Canada, Geological Association of Canada, IV. Series: GEOText; 6, pp. 167-199.

Rainwater, E.H., 1960, Stratigraphy and its role in the future exploration for oil and gas in the gulf coast: Gulf Coast Association of Geological Societies, v. X, p. 33-75.

Rider, Malcom, 1996, The geological interpretation of well logs, Latheronwheel, Caithness, UK, Whittles Publishing, 280 p.

Snedden, John W., 2010, A compilation of Phanerozoic sea-level change, Coastal onlaps and recommended sequence designations: AAPG Abstract, Search and Discovery Article #40594, p. 1-3

Snedden, John W., and Robert W. Dalrymple, 1999, Modern shelf sand ridges: From historical perspective to a unified model: SEPM Special Publication No. 64, p. 13-28.

Snedden, John W., and Katherine M. Bergmann, 1999, Isolated shallow marine sand bodies: Deposits for all interpretations: SEPM Special Publication No. 64, p. 1-11.

Stephenson, Llyod W., 1941, Summary of faunal studies of Navarro Group of Texas: AAPG Bulletin, v. 25, p. 637-643.

Stonecipher, Sharon A., 1999, Genetic characteristics of glauconite and siderite: Implications for the origin of ambiguous isolated marine sand bodies: SEPM Special Publication No. 64, p. 55-84.

Swift, Donald J.P., and Brian S. Parsons, 1999, Shannon sandstone of the Powder River basin: Orthodoxy and revisionism is stratigraphic thought: SEPM Special Publication No. 64, p. 191-204.

Texas State Railroad Commission, 2006, Annual report of the oil and gas division, 2007, v. I: Austin, Texas, 243 p.

APPENDIX A

Drill Cutting Sediment Descriptions

Sample #	Description
KC (1)	Dark to medium gray silt, poorly to moderately sorted with lower very coarse to upper medium sand, angular to sub-rounded, abundant amounts of ostracods, gastropods, *Lenticulina* and shell fragments, small hard shale and limestone fragments and pyrite concretions.
KC (2)	Light gray silty clay, lower very coarse to upper medium sand, angular to sub-rounded, hard fragments of shale and limestone with abundant amounts of ostracods, gastropods, shell fragments and *Lenticulina*.
KC (3)	Light gray silty clay, lower very coarse to upper medium sand, angular to sub-rounded, hard fragments of shale and limestone with ostracods, gastropods, shell fragments and *Lenticulina*.
KC (4)	Light gray silty clay, lower very coarse to upper medium sand, angular to sub-rounded, hard fragments of shale and limestone with ostracods, gastropods, shell fragments and *Lenticulina*.
KC (5)	Light gray silty clay, lower very coarse to upper medium sand, angular to sub-rounded, with ostracods, gastropods, shell fragments and low amounts of *Lenticulina* and pyrite inclusions.
KC (6)	Dark to medium brownish gray silt, poor to moderately sorted with lower very coarse to upper medium sand, angular to sub-rounded, with ostracods, gastropods, shell fragments and low amounts of *Lenticulina*.
KC A-3 (1)	Dark to medium brownish gray silt, poor to moderately sorted with abundant amounts of lower very coarse to upper medium sand, angular to sub-rounded, with ostracods, gastropods, shell fragments, low amounts of *Lenticulina*, hard shale fragments and pyrite inclusions.
KC A-3 (2)	Dark to medium brownish gray silt, poor to moderately sorted with abundant amounts of lower very coarse to upper medium sand, angular to sub-rounded, with ostracods, gastropods, echinoid spines, worm tubes???, shell fragments and low amounts of *Lenticulina*.
KC A-3 (3)	Dark to medium brownish gray silt, poor to moderately sorted with abundant amounts of lower very coarse to upper medium sand, angular to sub-rounded, with ostracods, gastropods, shell fragments and low amounts of *Lenticulina*.
KC A-3 (4)	Dark to medium brownish gray silt, poor to moderately sorted with abundant amounts of lower very coarse to upper medium sand, angular to sub-rounded, with ostracods, gastropods, shell fragments and low amounts of *Lenticulina*.
KC A-3 (5)	Dark to medium brownish gray silt, poor to moderately sorted with lower very coarse to upper medium sand, angular to sub-rounded, with ostracods, gastropods, shell fragments and low amounts of *Lenticulina*.

KC A-2 (1) Dark to medium brownish gray silt, poor to moderately sorted with lower very coarse to upper medium sand, angular to sub-rounded, with ostracods, gastropods, shell fragments, low amounts of *Lenticulina* and pyrite inclusion.

KC A-2 (2) Dark to medium brownish gray silt, poor to moderately sorted with lower very coarse to upper medium sand, angular to sub-rounded, with ostracods, gastropods, shell fragments and low amounts of *Lenticulina*.

KC A-1 (1) Dark to medium gray silt, poorly to moderately sorted with sparse amounts lower very coarse to upper medium sand, angular to sub-rounded, low amounts of ostracods, gastropods, *Lenticulina* and shell fragments, and pyrite concretions.

KC A-1 (2) Dark to medium gray silt, poorly to moderately sorted with lower very coarse to upper medium sand, angular to sub-rounded, abundant amounts of ostracods, gastropods, *Lenticulina* and shell fragments, small hard shale and limestone fragments, hydrocarbon fragments and low amounts of pyrite inclusions.

KC A-1 (3) Dark to medium gray silt, poorly to moderately sorted with lower very coarse to upper medium sand, angular to sub-rounded, abundant amounts of ostracods, gastropods, *Lenticulina* and shell fragments, small hard shale and limestone fragments and pyrite concretions.

KC A-1 (4) Light to medium gray marl, very fine silt, moderately sorted with sparse lower coarse to upper medium sand, muscovite mica, low amounts of ostracods, *Lenticulina*, shell fragments, hard shale fragments.

KC A-1 (5) Light to medium gray marl, very fine silt, moderately sorted with sparse lower coarse to upper medium sand, muscovite mica, low amounts of ostracods, *Lenticulina*, shell fragments, hard shale fragments.

KC A-1 (6) Light to medium gray marl, very fine silt, moderately sorted with sparse lower coarse to upper medium sand, muscovite mica, low amounts of ostracods, *Lenticulina*, shell fragments, hard shale fragments.

KC A-1 (7) Light to medium gray marl, very fine silt, moderately sorted with sparse lower coarse to upper medium sand, muscovite mica, some black fragments composing of inoceramids, organic plant matter, abundant amounts of ostracods, *Lenticulina*, gastropods, shell fragments, hard shale fragments.

KC B-4 (1) Light to medium gray marl, very fine silt, moderately sorted with sparse lower coarse to upper medium sand, ostracods, gastropods, shell fragments, hard shale fragments, *Lenticulina*, and small pyrite inclusions.

KC B-4 (2) Light to medium gray marl, very fine silt, moderately sorted with sparse lower coarse to upper medium sand, ostracods, gastropods, echinoid spines, worm tube???, shell fragments, and *Lenticulina*.

KC B-4 (3) Light to medium gray marl, very fine silt, moderately sorted with sparse lower coarse to upper medium sand, abundant amounts of ostracods, gastropods, *Lenticulina* and shell fragments, and hard shale fragments.

KC B-4 (4)	Light to medium gray marl, very fine silt, moderately sorted with sparse lower coarse to upper medium sand, ostracods, gastropods, shell fragments, hard shale fragments, and *Lenticulina*.
KC B-3 (1)	Light to medium gray marl, very fine silt, moderately sorted with sparse lower coarse to upper medium sand, parse ostracods and shell fragments, hard shale fragments, and pyritized inclusions.
KC B-2 (1)	Light to medium gray marl, very fine silt, moderately sorted with sparse lower coarse to upper medium sand, ostracods, gastropods, shell fragments, hard shale fragments, *Lenticulina* and pyritized molds.
KC B-2 (2)	Light to medium gray marl, very fine grained silt, moderately well sorted with *Lenticulina*, shell fragments and poorly cemented with calcite.
KC B-1 (1)	Light to medium gray marl, very fine silt, moderately sorted with sparse lower coarse to upper medium sand, ostracods, gastropods, shell fragments, hard shale fragments, *Lenticulina* and pyritized molds.
KC B-1 (2)	Light to medium gray marl, very fine grained silt, moderately well sorted with *Lenticulina*, shell fragments and poorly cemented with calcite.
KC B-1 (3)	Light to medium gray marl, very fine grained silt, moderately well sorted with *Lenticulina*, gastropods, shell fragments and poorly cemented with calcite.
KC B-1 (4)	Light to medium gray marl, very fine grained silt, moderately well sorted with *Lenticulina*, shell fragments and poorly cemented with calcite.
KC B-1 (5)	Light to medium gray marl, very fine grained silt, moderately well sorted with *Lenticulina*, shell fragments and poorly cemented with calcite.
KC B-1 (6)	Light to medium gray marl, very fine grained silt, moderately well sorted with *Lenticulina*, increased amount of shell fragments, and poorly cemented with calcite.
KC B-1 (7)	Light to medium gray marl, very fine grained silt, moderately well sorted with *Lenticulina*, shell fragments and poorly cemented with calcite.
KC B-1 (8)	Light to medium gray marl, very fine grained silt, moderately well sorted with lower amounts of shell fragments and *Lenticulina*, pyrite concretions and poorly cemented with calcite.
KC B-1 (9)	Light to medium gray marl, very fine grained silt, moderately well sorted with lower amounts of shell fragments and *Lenticulina*, pyrite concretions and poorly cemented with calcite.
KC B-1 (10)	Light to medium gray marl, very fine grained silt, moderately well sorted with *Lenticulina*, pyrite concretions and poorly cemented with calcite.
KC B-1 (11)	Light gray to white marl, very fine silt sized grains, well sorted, poor cementation with calcite.
KC B-1 (12)	Light to medium gray marl, very fine grained silt, moderately well sorted with some hard shale fragments and *Lenticulina*, shell fragments, pyrite concretions and poorly cemented with calcite.
KC B-1 (13)	Medium to dark gray marl, fine grained silt, moderately well sorted that is poorly cemented with calcite, lower calcite content due to lower reaction with HCL, contains hard shale fragments both light and dark brownish

	red, shell fragments observed and very sparse fine grained sand with pyrite concretions.
KC B-1 (14)	Light gray marl, fine grained silt, moderately well sorted that is poorly cemented with calcite, contains hard shale fragments both light and dark brownish red, shell fragments observed and very sparse fine grained sand with pyrite concretions.
KC B-1 (15)	Light gray marl, fine grained silt, moderately well sorted that is poorly cemented with calcite, contains hard shale fragments both light and dark brownish red, shell fragments observed and very sparse fine grained sand with pyrite concretions.
KC B-1 (16)	Light gray marl, fine grained silt, moderately well sorted that is poorly cemented with calcite, contains hard shale fragments both light and dark brownish red, shell fragments observed and very sparse fine grained sand with pyrite concretions.
CM (1)	Light gray to white marl, very fine grained silt, moderately well sorted with poor cementation that is calcite and reacts with acid more readily then CM (2) sample.
CM (2)	Medium gray marl, well sorted, poor to no cementation with very few *Lenticulina* and has very low amounts of calcite compared to CM (1&3) observed by lack of interaction with HCl test.
CM (3)	Dark gray marl, fine grained, well sorted poorly cemented with large quantities of calcite and *Lenticulina* fossils found in sample along with coarse grains of sand scattered throughout.
CM (4)	Dark gray marl, fine grained, well sorted poorly cemented with large quantities of calcite and *Lenticulina* fossils found in sample.
CM (5)	Dark gray marl, fine grained, well sorted poorly cemented with large quantities of calcite and has some type of seeds covered in a white crust that could b contamination from the surface during drilling operations.
NAC (1)	Dark gray marl, fine grained, well sorted poorly cemented with large quantities of calcite.
NAC (2)	Dark gray marl, fine grained, well sorted poorly cemented with large quantities of calcite.
NAC (3)	Dark gray marl, fine grained, well sorted poorly cemented with large quantities of calcite and has some glauconite and lithic fragments (black).
NAC (4)	Light gray to white marl, very fine gained sub-rounded to rounded with poor cementation that is highly calcitic.
NAC (5)	Light gray to white marl, very fine gained sub-rounded to rounded with poor cementation that is highly calcitic and some black fragments composing of inoceramids, organic plant matter.
NAC (6)	Medium gray silt, fine grained, moderately sorted, well rounded with glauconite, muscovite mica, calcite and black fragments composing of inoceramids, echinoid spines, organic plant matter and hydrocarbon.

NAC (7)	Medium gray silt, fine grained, moderately sorted, well rounded with glauconite, muscovite mica, calcite and black fragments composing of inoceramids, echinoid spines, organic plant matter and hydrocarbon.
NAC (8)	Medium gray sand, medium to coarse grained, moderately sorted, sub-rounded to sub-angular with pyrite nodules, glauconite, muscovite mica, calcite and black fragments composing of inoceramids, echinoid spines, organic plant matter and hydrocarbon.
NAC (9)	Medium gray sand, medium to coarse grained, moderately sorted, sub-rounded to sub-angular with pyrite nodules, glauconite, muscovite mica, calcite and black fragments composing of inoceramids, echinoid spines, organic plant matter and hydrocarbon.
NAC (10)	Medium gray sand, medium to coarse grained, moderately sorted, sub-rounded to sub-angular with pyrite nodules, glauconite, muscovite mica, calcite and black fragments composing of inoceramids, echinoid spines, organic plant matter and hydrocarbon.
NAC (11)	Medium gray sand, medium to coarse grained, moderately sorted, sub-rounded to sub-angular with pyrite nodules, glauconite, muscovite mica, calcite and black fragments composing of inoceramids, echinoid spines, organic plant matter and hydrocarbon.
NAC (12)	Medium gray sand, medium to coarse grained, moderately sorted, sub-rounded to sub-angular with pyrite nodules, glauconite, muscovite mica, calcite and black fragments composing of inoceramids, echinoid spines, organic plant matter and hydrocarbon.

APPENDIX B

Facies Descriptions from Sediments

Sandstone Facies **(NAC [8] – NAC [12])**

Medium gray sand, medium to coarse grained, moderately sorted, sub-rounded to sub-angular with pyrite nodules, glauconite, muscovite mica, calcite and black fragments composing of inoceramids, echinoid spines, organic plant matter and hydrocarbon.

Marl Facies **(KC A-1 [4] – NAC [5])**

Light, dark gray to white marl, very fine gained sub-rounded to rounded with poor cementation that is highly calcitic and some black fragments composing of inoceramids, organic plant matter.

Siltstone Facies **(NAC [6] – NAC [7]) / (KC [6] – KC A-1 [3])**

Dark to medium gray silt, poorly to moderately sorted with lower very coarse to upper medium sand, angular to sub-rounded, abundant amounts of ostracods, gastropods, *Lenticulina* and shell fragments, small hard shale and limestone fragments, hydrocarbon fragments and low amounts of pyrite inclusions.

Clays Facies **(KC [2] – KC [5])**

Light gray silty clay, lower very coarse to upper medium sand, angular to sub-rounded, hard fragments of shale and limestone with abundant amounts of ostracods, gastropods, shell fragments and *Lenticulina*.

APPENDIX C

County	Well Name	Longitude	Latitude
Falls	HUGH T. HAY #1	-96.76802	31.18857
Milam	BLANCHE M #2	-96.78276	30.78927
Milam	COFFIELD #1	-96.7886	30.70616
Milam	McCrary #1	-96.763335	30.978102
Milam	McCrary #2	-96.760784	30.978712
Milam	McCrary #4	-96.759836	30.981105
Milam	MCCREARY #1	-96.767222	30.929298
Milam	MCCRARY & BRECK #8	-96.75581	30.99843
Milam	MCCRARY & BRECK #10	-96.75783	30.9958
Milam	MCCRARY & BRECK #11	-96.75624	30.99952
Milam	MCCRARY & BRECK #18	-96.75689	30.99447
Milam	MCCRARY & BRECK #19	-96.74884	31.00039
Milam	PAGE #1	-96.79545	30.68623
Milam	Patksie #1	-96.763984	30.955691
Milam	SMITH #1	-96.725305	30.883732
Roberson	A. J. SMITH 2-1	-96.72861	30.87541
Robertson	B. J. WILKINSON T-BAR-X	-96.433745	30.967762
Robertson	BURNITT #3	-96.71559	30.996498
Robertson	BURNITT, PAULINE D. #3	-96.7251	30.98766
Robertson	CRISTINA #1	-96.719221	30.99154
Robertson	FNB UNIT #1	-96.35004	31.0063
Robertson	Garrett #1	-96.757381	30.950924
Robertson	Garrett #2	-96.754547	30.950381
Robertson	Garrett #3	-96.754888	30.947783
Robertson	Garrett #4	-96.753598	30.952864
Robertson	Garrett #5	-96.75159	30.953949
Robertson	Garrett #6-A	-96.749777	30.956046
Robertson	Garrett #7	-96.7517	30.952207
Robertson	Garrett #8	-96.755204	30.953344
Robertson	Gibson #1	-96.755556	30.956836
Robertson	Gibson #1-A	-96.741186	30.971642
Robertson	Gibson #2	-96.753363	30.958209
Robertson	Gibson #3	-96.757786	30.955753
Robertson	Gibson #4	-96.754613	30.954855
Robertson	Gibson #5	-96.753972	30.960996
Robertson	Gibson #6	-96.757281	30.962211
Robertson	Gibson #7	-96.756495	30.95937
Robertson	Gibson #8	-96.759279	30.963795
Robertson	Gibson #9	-96.759613	30.960815
Robertson	Gibson #10	-96.762256	30.96224
Robertson	Gibson #11	-96.761964	30.959446
Robertson	Gibson #12	-96.759009	30.958253
Robertson	Gibson #13	-96.763695	30.961546
Robertson	Gibson #14	-96.759752	30.97053
Robertson	Gibson #15	-96.759398	30.968006
Robertson	Gibson #16	-96.760764	30.965677
Robertson	Gibson #17	-96.763351	30.964385

County	Well Name	Longitude	Latitude
Robertson	Gibson #18	-96.757547	30.965618
Robertson	Gibson #19	-96.76191	30.969617
Robertson	Gibson #20	-96.761352	30.967784
Robertson	Gibson #21	-96.761623	30.960665
Robertson	Gibson #22	-96.76083	30.958988
Robertson	Gibson #23	-96.761264	30.964305
Robertson	Gibson #24	-96.758334	30.956687
Robertson	Gibson #25	-96.75303	30.968245
Robertson	Gibson #26	-96.755678	30.959721
Robertson	Gibson #27	-96.757969	30.961814
Robertson	Gibson #30	-96.739261	30.970525
Robertson	Gibson #31	-96.7629	30.9649
Robertson	Gibson #32	-96.767947	30.964681
Robertson	Gray No.1	-96.572915	30.990431
Roberston	MCCRARY & BRECK #12	-96.75584	30.99556
Robertson	MISCHSER #1	-96.33523	31.03275
Robertson	MOODY ESTATE #1	-96.6147	30.94332
Robertson	Norris #1	-96.768208	30.968427
Robertson	Norris #1-A	-96.757685	30.973909
Robertson	Norris #2-A	-96.760589	30.972334
Robertson	Norris #3-A	-96.760289	30.97466
Robertson	Norris #4	-96.761564	30.973459
Robertson	Norris #5	-96.762645	30.971331
Robertson	RACHUI #1	-96.45383	31.02982
Robertson	STAWNICZ #1	-96.26566	31.05783